https://doi.org/10.5194/egusphere-2023-860
Preprint. Discussion started: 30 May 2023

Observations of cyanogen bromide (BrCN) in the global troposphere and their relation to polar surface O_3 destruction.

James M. Roberts[1*], Siyuan Wang[1,2], Patrick R. Veres[1,3], J. Andrew Neuman[1,2], Michael A. Robinson[1,2], Ilann Bourgeois[1,2,4], Jeff Peischl[1,2], Thomas B. Ryerson[1,5], Chelsea R. Thompson[1], Hannah M. Allen[6], John D. Crounse[7], Paul O. Wennberg[7,8], Samuel R. Hall[9], Kirk Ullmann[9], Simone Meinardi[10], Isobel J. Simpson[10], and Donald Blake[10]

1. NOAA Chemical Sciences Laboratory, Boulder, CO, USA
2. Cooperative Institute for Research in Environmental Sciences, CIRES, University of Colorado, and NOAA, Boulder, CO, USA
3. now at Earth Observing Laboratory, National Center for Atmospheric Research, Boulder, CO, USA
4. now at Université Savoie Mont Blanc, INRAE, CARRTEL, F-74200 Thonon-Les Bains, France.
5. now at Scientific Aviation, Boulder, CO., USA
6. Division of Chemistry and Chemical Engineering, California Institute of Technology, Pasadena, CA, USA
7. Division of Geological and Planetary Sciences, California Institute of Technology, Pasadena, CA, USA
8. Division of Engineering and Applied Science, California Institute of Technology, Pasadena, CA, USA
9. Atmospheric Chemistry Observations & Modeling Laboratory, National Center for Atmospheric Research, Boulder, CO, USA
10. Department of Chemistry, University of California Irvine, Irvine, CA, USA.

Correspondence to: James.M.Roberts@noaa.gov

Abstract. Active bromine (e.g., Br_2, BrCl, BrO, HOBr) promotes atmospheric ozone destruction and mercury removal. Here we report a previously unidentified participant in active-Br chemistry, cyanogen bromide (BrCN), measured during the NASA Atmospheric Tomography (ATom) mission. BrCN was confined to polar boundary layers, often appearing at concentrations higher than other Br compounds. The chemistry of BrCN determines whether it promotes or inhibits ozone and mercury removal. This dataset provides evidence that much of the BrCN was from atmospheric Br chemistry involving surface reactions with reduced nitrogen compounds. Since gas phase loss processes are known to be relatively slow, surface reactions must also be the major loss processes, with vertical profiles implying a BrCN atmospheric lifetime in the range 1–10 days. Liquid phase reactions of BrCN tend to convert Br to bromide (Br^-) or C-Br bonded organics, constituting a loss of active Br. Thus, accounting for BrCN chemistry is crucial to understanding polar Br cycling.

1 Introduction

Photochemically-active halogen species in the lower troposphere affect the oxidizing capacity of the atmosphere via radical reactions that may either produce or destroy ozone. In addition, active halogens play an important role in O_3 destruction when transported to the upper troposphere and lower stratosphere (UT/LS). Active-halogen species are defined as halogen

https://doi.org/10.5194/egusphere-2023-860
Preprint. Discussion started: 30 May 2023

atoms, dihalogen compounds, or species that have an effective oxidation state above -1, (e.g., hypobromous acid, HOBr). A complete understanding of this chemistry requires an accounting of reactions that produce or destroy active halogens in a variety of environments, ranging from the polar icecaps, the ocean surface layer, and polluted continental regions.

Bromine chemistry in polar surface regions has been of particular interest since it was discovered that active-bromine compounds were responsible for ozone destruction in those regions (Barrie et al., 1988). The chemistry behind the initiation and propagation of active-bromine chemistry has since been the subject of numerous experimental and numerical modeling studies and several review articles (Abbatt et al., 2012;Simpson et al., 2015;Simpson et al., 2007), and ozone destruction is a widespread and persistent phenomenon in the Arctic boundary layer (Jacobi et al., 2010). Ozone destruction follows from the production of Br_2 or BrCl on ice, snow or particle surfaces, volatilization into the gas phase, and subsequent photolysis to two halogen atoms that react rapidly with O_3 to create halogen oxide (XO, where X = Cl, Br, or I). Halogen oxides have number of pathways to form hypohalous acids (HOX) that can amplify the halogen chemistry through surface reactions with halide ions, for example:

$$HOBr + Br^- + H^+ \rightarrow Br_2 + H_2O \quad (R1)$$

This phenomenon has been termed the "bromine explosion" when it accompanies the destruction of ozone (Wennberg, 1999;Platt and Janssen, 1995). One of the keys to achieving a quantitative understanding of this Br chemistry is assessing the other heterogeneous reactions that HOBr can participate in. For example, there is evidence that HOBr reacting with dissolved organic matter (DOM), either on surface snow/ice or on particles, could be responsible for bromoform ($CHBr_3$) enhancements observed in polar environments (Carpenter et al., 2005;Gilman et al., 2010) and $CHBr_3$ and other organic bromine compounds observed in sea ice in the Antarctic winter (Abrahamsson et al., 2018). Reaction of HOBr with reduced nitrogen species to form cyanogen bromide (BrCN) could divert active bromine from the O_3 bromine explosion cycle.

The existence of cyanogen halides has been known for some time (e.g., ClCN was discovered in 1851 (Wurtz, 1851)), but to our knowledge they have not been reported in the ambient atmosphere. Note that cyanogen fluoride (FCN) is known, but FCN will not be formed in the environment due to the lack of chemical pathways that can form active F (e.g. HOF, F_2). In the environment, XCN compounds are formed from the reaction of active halogens, X_2, or HOX (where = Cl, Br, I) with reduced nitrogen species. For example,

$$X_2\ (HOX) + HCN \rightarrow XCN + HX\ (H_2O) \quad (R2)$$

This chemistry is well known in water and wastewater treatment processes where Cl_2, NaOCl or chloramines are added and reduced nitrogen species are present (Shah and Mitch, 2012;Yang and Shang, 2004). ClCN, and to some extent BrCN, has been measured in chlorination systems, including swimming pools and spas (Daiber et al., 2016) and water treatment systems (Heller-Grossman et al., 1999), because the reaction of active-Cl compounds with bromide ions produces active Br. For example:

$$HOCl + Br^- \rightarrow HOBr + Cl^- \quad (R3)$$

As in the case of Cl chemistry, a range of N-containing substrates may be involved in BrCN formation. The solubility of XCN compounds has recently been found to range from only slightly soluble for ClCN to moderately soluble for ICN (Roberts and

https://doi.org/10.5194/egusphere-2023-860
Preprint. Discussion started: 30 May 2023

Liu, 2019). Thus, cyanogen halides will easily volatilize from solution and should be considered as possible important participants in active-halogen chemistry in the troposphere.

In addition to the above purely abiotic mechanisms, ClCN, BrCN and ICN are known to be produced in biological systems through photosynthetic reactions involving H_2O_2, halides, and peroxidase enzymes present in neutrophils or other simple organisms (Vanelslander et al., 2012;Zgliczynski and Stelmaszynska, 1979;Schlorke et al., 2016). In those systems superoxide and hydrogen peroxide (O_2^-/H_2O_2) are used by enzymes to produce HOX compounds, and then XCN compounds by further reaction with N-containing substrates. In fact, there is evidence that several species of marine diatom have evolved to produce BrCN, and to some extent ICN, through photosynthetic production of H_2O_2 and its conversion to HOX and then XCN compounds, by bromo- and iodo-peroxidases (Vanelslander et al., 2012). One hypothesis is that microalgae have evolved this capability because BrCN suppresses other competing marine microbiota in marine biofilm communities (Vanelslander et al., 2012). Thus, cyanogen halides and BrCN in particular could have both biotic and abiotic sources, linked through common chemical mechanisms: the reactions of HOBr with reduced-N compounds either in marine organisms and biofilms, or on ice/snow and particles in the polar boundary layer.

The co-production of the bromomethanes, dibromomethane (CH_2Br_2) and $CHBr_3$ by marine microalgae can be used to distinguish between biotic (marine) and abiotic BrCN sources. Laboratory and field measurements show that marine CH_2Br_2 and $CHBr_3$ are co-products of the bromo-peroxidase process operating in marine diatoms (Mehlmann et al., 2020;Moore et al., 1996;Hughes et al., 2013), with $CHBr_3$ the primary product of peroxidase-HOBr chemistry, and CH_2Br_2 formed from $CHBr_3$ by bacterial action (Hughes et al., 2013). Abiotic HOBr chemistry, including water disinfection processes, produces $CHBr_3$ predominately (Maas et al., 2019;Mehlmann et al., 2020), so elevated $CHBr_3$ relative to CH_2Br_2 would be a marker for the atmospheric chemistry that initiates and perpetuates the bromine explosion. This aspect is borne out by the observations of organic bromine compounds in the Antarctic winter (i.e. in the absence of photosynthesis) where $CHBr_3$/CH_2Br_2 ratios were often 10 or higher (Abrahamsson et al., 2018). The source of active bromine in (Abrahamsson et al., 2018) was hypothesized to be the dark reaction of ozone with bromide-containing solutions or ice, a process for which there is substantial experimental evidence (Artiglia et al., 2017;Oum et al., 1998;Sakamoto et al., 2018;Clifford and Donaldson, 2007).

The atmospheric loss processes of XCN compounds have not been studied extensively, but there are some limits that can be placed on them. Reactions of the radicals OH and Cl atoms with XCN compounds are likely quite slow ($<10^{-13}$ cm^3/molecule-s) because any direct abstraction reactions (e.g. OH + BrCN $\rightarrow$ HOBr + CN) are highly endothermic, and addition reactions to the -CN group are expected to be quite slow by analogy to HCN and CH_3CN reactions. XCN photolysis has been estimated to range from no tropospheric photolysis of ClCN, to a BrCN photolytic lifetime of ≅135 days, to an ICN lifetime of ≅9 hrs at summer time mid-latitudes (Fig. S1). The solubility and hydrolysis rates of XCN compounds have been measured under a variety of conditions (Roberts and Liu, 2019). Solubilities of ClCN and BrCN are relatively low (4.5 and 33 M/atm at 273K, respectively), and their hydrolysis reactions are base-catalyzed and relatively slow at ambient pHs ($<1 \times 10^{-5}$ s^{-1} at 273K). The net effect of these features is that while ICN can photolyze relatively readily, ClCN and BrCN removal from

https://doi.org/10.5194/egusphere-2023-860
Preprint. Discussion started: 30 May 2023

the troposphere is likely governed by heterogeneous uptake and reaction with materials in those matrices, whether that be aerosol, cloud, or surfaces.

There have been almost no reported observations of XCN compounds in the gas phase in environmental systems in spite of the facile chemistry that forms XCN compounds in aquatic chemistry. ClCN has been observed by proton-transfer reaction high-resolution time of flight mass spectrometry (Mattila et al., 2020) in indoor air during experiments in which a home was cleaned with chlorine bleach solution, but to our knowledge, neither BrCN nor ICN have been observed previously in the atmosphere. Two factors may be responsible for the lack of ambient measurements of XCN compounds: (1) other chemical loss processes removing XCN species are likely much faster than hydrolysis, and (2) sensitive on-line analytical techniques for their measurement have only recently been available.

Here we report observations of BrCN in the global atmosphere during the second, third and fourth deployments of the NASA Atmospheric Tomography (ATom) experiment in January-February 2017, September-October 2017 and April-May 2018 (Thompson et al., 2022). The measurements were obtained aboard the NASA DC-8 research aircraft by trifluoromethoxide (CF_3O^-) chemical ionization with time-of-flight mass spectrometry detection (hereafter referred to as CIT-CIMS) during ATom-1,2,3&4 and by iodide ion chemical ionization with high resolution time-of-flight mass spectrometry (hereafter referred to as the I-CIMS) (Veres et al., 2020) during ATom-3&4. The I-CIMS was not deployed for ATom-1&2. The project also provided an extensive suite of co-measured species used to assess the relative role of biotic and abiotic BrCN production mechanisms. This paper summarizes the geographic distributions of BrCN, and presents several case studies of large BrCN enhancements. We then present evidence that shows a significant fraction of BrCN was produced from active-Br chemistry.

2 Experimental Methods

2.1 Experimental Design

The ATom experiment was an extensive project, with a wide-ranging set of chemical and physical measurements during four separate season deployments aboard the NASA DC-8 research aircraft. An overview of the ATom mission has been given elsewhere(Thompson et al., 2022), so only aspects pertinent to this work will be discussed here. Two instruments detected BrCN during the ATom deployments; a time-of-flight mass spectrometer that employed trifluoromethoxide (CF_3O^-) ionization (CIT-CIMS) flew during all four deployments and a high-resolution time-of-flight mass spectrometer that employed iodide ion ionization (I-CIMS) flew only on the 3rd and 4th global circuits (ATom-3&4) in October 2017 and May 2018. The aircraft sampled the troposphere from 86°S to 83°N in more than 180 vertical profiles in each mission interspersed with level legs that ranged in altitude from about 0.150 to 13.2 km, with MAs over Arctic airports as low as 0.043 km.

2.2 I-CIMS

https://doi.org/10.5194/egusphere-2023-860
Preprint. Discussion started: 30 May 2023

The measurement of BrCN during ATom-3&4 was accomplished using a high-resolution time-of-flight mass spectrometer (Aerodyne Research, Billerica, Massachusetts) that employed iodide ion adduct ionization chemistry. The instrumental conditions were described by Veres et al., (2020), and included control of pressure and water vapor concentration in the ion-molecule reaction (IMR) region. The resolving power of the mass spectrometer was approximately 5000 (m/Δm) in the mass range of interest. This resolving power, coupled with the negative mass defect of Br yields a clear signal for BrCN, even for relatively small amounts (5.3 pptv) as shown in Fig 1. BrCN is detected as the I^- adducts, $I{\bullet}Br^{79}CN^-$ and $I{\bullet}Br^{81}CN^-$, and those ions were well separated from other ions that appear at the same nominal mass. The combination of mass separation and isotope relative abundance provides conclusive identification of BrCN. The instrument background for the BrCN signal was determined by overflowing the instrument inlet with scrubbed ambient air every 8 minutes for a 30 second period, and the detection limit of the measurements was determined by the variability in the residual signal at that mass.

Calibration of the XCN compounds was accomplished using the method described by Roberts and Liu (2019) following the ATom-3 deployment. ClCN was produced by conversion of a calibrated mixture of HCN in air to ClCN in a reactor containing Chloramine-T (*N*-Chloro-*p*-toluenesulfonamide sodium salt). The concentration of this calibrated stream was verified by a Total Reactive Nitrogen (N_r) instrument (Stockwell et al., 2018) to be in the range of tens of ppbv at the CIMS inlet flow rates and the presence of ClCN confirmed by analysis with a high-resolution proton-transfer-reaction time-of-flight mass spectrometer (Hi-Res-PTR-ToF). The I-CIMS had no discernable response to ClCN at $I{\bullet}ClCN^-$ or potential fragment ions. A similar absence of sensitivity to ClCN was also found in a study of indoor air chemistry during chlorine bleach treatment (Mattila et al., 2020), where a PTR-MS was able to observe ClCN but the I-CIMS deployed in the same study did not detect it (J. Mattila personal communication, 2020). Standard streams of BrCN and ICN were produced using the pure compounds (Sigma-Aldrich and Acros Organics, respectively) placed in diffusion cells and calibrated by the N_r instrument under constant temperature and pressure conditions. The conversion efficiency of the N_r catalyst was found to be 98±10% for ClCN and assumed to be the same for BrCN and ICN based on the X-CN bond energies of these molecules (Table S1). The IMR temperature was held constant at 40°C during the sensitivity determinations and for a majority of the ambient measurements. The temperature dependence of the I-CIMS sensitivity to BrCN was determined in the laboratory to be nearly identical to that of formic acid (Robinson et al., 2022), and was used to correct the data from the flights on Oct. 25, 2017 and Oct. 27, 2017 during which the IMR was operated at 45°C. The I-CIMS sensitivity was also found to decrease with increased IMR water vapor concentration. Response factors were then determined for the conditions corresponding to the ATom-3 and ATom-4 deployments. The I-CIMS was approximately 8× more sensitive to ICN compared to BrCN, which combined with the ClCN result gives I-CIMS relative sensitivities in the order ICN>BrCN>>ClCN. Clear signals for ICN were observed in ambient air at the $I{\bullet}ICN^-$ product ion, but the large instrument backgrounds caused by the use of iodide as the reagent ion prevented quantitation of ICN. Generally, detection limits of 1.5 pptv (3× standard deviation of the signal at zero BrCN) for a 10 s average with overall uncertainties of 0.4 pptv +25%, as calibrated, pertain to most measurements, with the exception of

https://doi.org/10.5194/egusphere-2023-860
Preprint. Discussion started: 30 May 2023

the flights during ATom-4 on May 12, May 17, and May 21, 2018, during which the detection limit was 6 pptv for 10 s averages, due to increased water vapor in the IMR and corresponding decreased sensitivity.

The instrument time response for BrCN was found to be fast (τ~1.5 s) both during calibration experiments and in assessing the time variability of signal attributed to ambient BrCN. This fast response is consistent with the measured Henry's Law constant of BrCN and our understanding of the absorptive behavior of polar and inorganic gases on PFA inlets (Liu et al., 2019).

The potential formation of BrCN on the inlet surfaces of the instrument needs to be considered since it might involve the same chemistry that is making BrCN in the environment, i.e. the reaction of HOBr with reduced-N species on inlet surfaces. Several pieces of evidence indicate a lack of any BrCN production in our system. First, calibrations of the instrument with Br_2 and BrO standards before and after these missions did not result in any observable BrCN above detection limit. Second, the solubility, and therefore surface concentration, of HCN (a likely reaction partner) is quite low at the temperature at which the inlet was operated (40°C). In contrast, the inlet is more likely to collect non-volatile Br^- and convert HOBr to Br_2, as demonstrated by previous measurements in the Arctic troposphere (Neuman et al., 2010). As noted above, both of these heterogeneous processes are also pH dependent, and Br_2 will be much more favored at lower pHs that are likely present in the surface layers of the PFA inlet (Nault et al., 2020).

Several other halogen species were measured with good sensitivity by the I-CIMS as their I^- adducts: Cl_2, $ClNO_2$, BrCl, and BrO (see Table S2). Calibrations of the I-CIMS for those species has been described (Neuman et al., 2010;Osthoff et al., 2008). Previous work has shown that Br_2 and HOBr measurements are not reliable with the inlet used on the aircraft due to interconversion reactions noted above (Neuman et al., 2010), so those species were not quantified.

2.3 CIT-CIMS.

HCN was measured by the Caltech chemical ionization mass spectrometer using CF_3O^- reagent ion. HCN forms a cluster ion with CF_3O^- and is detected at m/z 112. HCN was calibrated before and after each ATom deployment and a temperature and water-dependent sensitivity was used to convert the signal at m/z 112 to HCN concentrations after accounting for instrumental backgrounds determined by periodic zero measurements. BrCN was also detected by CIT-CIMS as CF_3O^- cluster ions at m/z 190 and 192. The signal at m/z 192 occasionally contained contributions from other molecules – signals that do not appear at m/z 190. Thus, m/z 190 signal was used for quantifying BrCN, dividing the signal by its isotopic abundance of ^{79}Br (0.51) due to the calibration method employed. When the signal at m/z 190 was elevated, the enhancement at m/z 192 was as well, reflecting the approximately equal abundance of ^{79}Br and ^{81}Br Independent BrCN temperature- and water-vapor dependent calibration factors for CIT-CIMS were determined in the Caltech laboratory using simple manometry in combination with FTIR spectroscopy. Five IR spectra with varying BrCN concentrations were collected as part of the calibration, and compared to the sum of the MS signals at m/z 190 and 192. An integrated absorption cross-section for the band centered at 2198 cm^{-1} was determined (2110–2250 cm^{-1} band: 1.08×10^{-18} cm $molec^{-1}$, log base-e at 298K). To the extent that other gases are present in the BrCN vapor sample, the integrated IR cross-section and the CIMS sensitivity represent lower

https://doi.org/10.5194/egusphere-2023-860
Preprint. Discussion started: 30 May 2023

limits, and in turn derived ambient concentrations represent upper limits. The 1-sigma BrCN precision for CIT-CIMS 10 s data, as calibrated, is 2.5 pptv.

Ambient BrCN mixing ratios from CIT-CIMS were compared with those from I-CIMS for two ATom-4 flights with the highest BrCN: Apr. 27, 2018, and May 19, 2018. The BrCN mixing ratios from the CIT-CIMS are scattered against those from the I-CIMS in Fig. S2a for the entire two flights and in Fig. S2b from the data points for which the I-CIMS mixing ratio was > 3pptv. The data in Fig. S2b were fit using an orthogonal-distance regression (ODR) that assumes uncertainty in both variables. The slope of the correlation of CIT-CIMs versus I-CIMS is 0.52 ±0.01 and the intercept is -0.341. At this point it is not possible to privilege one calibration method and data set over the other, so they were harmonized by correcting the two data sets to the mean. Accordingly, the I-CIMS data were multiplied by 0.76 and the CIT-CIMS data were multiplied by 1.46. As a result, the correct uncertainties of the I-CIMS BrCN measurements were 0.3pptv + 50%, with detection limit of 1.1 pptv, and the 10 s precision of the CIT-CIMs measurements was 3.7 pptv. The I-CIMS data have approximately 5× better signal-to-noise than the CIT-CIMS. Consequently, the I-CIMS data are used in the analyses of the ATom-3&4 flights, and the CIT-CIMS data are used in the analyses of the ATom-2 Arctic flights, the only other instances in which the CIT BrCN was above the detection limit.

2.4 Additional Measurements

2.4.1 NOxy and O_3 measurements.

The oxides of nitrogen: nitic oxide (NO), nitrogen dioxide (NO_2) and total odd nitrogen (NO_y), as well as O_3, were measured by a 4-channel chemiluminescence system as described previously (Bourgeois et al., 2021). The estimated uncertainties for these measurements, and instrument precision, are ±(5% + 6 pptv) for NO, ±(7% + 20 pptv) for NO_2, ±(12% + 15 pptv) for NO_y, and ±(2% + 15 pptv) for O_3.

2.4.2 Whole Air Sampler.

Bromoform ($CHBr_3$), dibromoethane (CH_2Br_2), methyl bromide (CH_3Br) and methyl iodide (CH_3I) were measured during ATom-2, 3 &4 using UC Irvine Whole Air Sampling (WAS). The WAS technique during airborne missions has been recently described by (Simpson et al., 2020). Briefly, air from outside the aircraft was drawn through a stainless steel manifold by a dual-head metal bellows pump into individual evacuated 2-L stainless steel canisters that were sequentially filled to a pressure of 40 psig (roughly 3 atm). Air samples were collected at the discretion of samplers on board the aircraft. The average canister fill time was 53 ±21 s (22–136 s) during ATom-2, 54 ±25 s (18–181 s) during, ATom-3 and 52 ±24 s (16–198 s) during ATom-4, and the average sampling frequency was every 2.6 minutes for all missions. A total of 303 samples were collected for the two Arctic legs of ATom-2, and 1933 and 1853 samples were collected during ATom-3 and ATom-4, respectively, for an average of 149 and 143 whole air samples per flight. The filled canisters were returned to UC Irvine and analyzed using multi-column gas chromatography. Complete analytical details and calibrations procedures are given in

https://doi.org/10.5194/egusphere-2023-860
Preprint. Discussion started: 30 May 2023

235 (Simpson et al., 2020). The measurement precision is 5% for CH_3I, CH_3Br and CH_2Br_2, and 10% for $CHBr_3$. The accuracy is 10% for CH_3Br and 20% for CH_3I, CH_2Br_2, and $CHBr_3$. The detection limit is 0.005 pptv for CH_3I, 0.5 pptv CH_3Br, and 0.01 pptv for CH_2Br_2 and $CHBr_3$.

2.4.3 UV-visible Actinic flux measurements.

240 Photolysis frequencies were determined from the Charged–coupled device Actinic Flux Spectroradiometers (CAFS) (Hall et al., 2018). Up and downwelling actinic flux is collected by 2 pi steradian optical collectors above and below the aircraft fuselage. The signals are directed via fiber optics to spectrometers to provide spectrally-resolved fluxes from 290–640 nm. The photolysis frequencies are then calculated by applying the total actinic fluxes to molecular cross sections and quantum yields contained in the Tropospheric Ultraviolet and Visible (TUV) radiative transfer model (v5.3) (Madronich and Flocke, 245 1999). Typical molecularly dependent uncertainties range from 12–20%.

2.5 Box Model Description

The model used to explore the formation of BrCN in the Arctic environment has been described previously (Wang and Pratt, 2017). It includes gas-phase, photolysis reactions, multi-phase reactions on both aerosol particles and snow, liquid-250 phase reactions in both deliquescent particles and liquid-like layers on snow and ice, dry deposition of trace gases. The liquid-phase reactions of active-bromine compounds with HCN/CN^- were added according to the reactions and rates specified in the Supplementary Material. The conditions and chemical measurements corresponding to the Apr. 27, 2018 missed approach over Utqiagvik, Alaska were used to initialize the model.

255 **2.6 Statistical Methods**

Statistical analyses were performed using the standard routines for averaging and ODR fitting provided by Igor Pro Version 8 software.

3 Results

The flight paths of the NASA DC-8 during ATom-2,3&4 provide a unique opportunity to assess the global extent of 260 BrCN, as those flight paths consisted of alternating high and low altitude legs around most of the global background troposphere with vertical profiles in between. The ATom-2 observations by the CIT-CIMS are limited to Arctic wintertime and will be presented below. Maps summarizing ATom-3&4 data from the I-CIMS instrument are shown in Fig. 2, where the flight paths are shown colored and sized by BrCN mixing ratios. BrCN mixing ratios ranged from below detection limit (1.1 pptv) up to 10 pptv for a 10 s average during ATom-3 and up to 36 pptv for a 10 s average during ATom-4. The highest BrCN 265 mixing ratios observed during ATom-3 occurred during the low-level legs that dipped into the boundary layer at high latitudes (below 65°S and above 65°N) and the remaining observations were at or below detection limit which was consistently 1.1 pptv for the ATom-3 campaign. Likewise, the highest mixing ratios observed during ATom-4 occurred during low level legs at high

https://doi.org/10.5194/egusphere-2023-860
Preprint. Discussion started: 30 May 2023

latitudes, but the degraded instrument sensitivity during the May 12, 17, and 21 flights (detection limit 4.6 pptv) resulted in greater variability at low mixing ratios on the ATom-4 map (Fig. 2b).

The vertical dependence of BrCN mixing ratios is explored further by plotting the observations as a function of altitude (Fig. 3a&b) with altitude plotted on log scales to enhance the details of the lowest altitudes. BrCN was confined to the polar boundary layer and inspection of the DC-8 camera footage, where available, shows that all of those legs were over ice, not over open ocean or bare land, although not every polar boundary layer leg had measurable BrCN. The only locations where the aircraft was lower than 150m were takeoffs or landings and at coastal airports and during a missed approach (MA) over BRW, the airport at Utqiagvik, AK. The BRW MA during ATom-3 did not show elevated BrCN, or other indicators of halogen activation, as described below. The highest BrCN mixing ratios during ATom-3 reached 10 pptv and occurred over the Arctic on Oct. 25, 2017. Details of some of the individual flights highlighted in Fig. 3a are described in Section 3.1. The vertical profiles from ATom-4 (Fig. 3b) show that the highest BrCN was observed during the MA over BRW, where it was clear that the aircraft entered the polar boundary layer. The other flights for which there was enhanced BrCN involved a combination of situations where the aircraft either reached the polar boundary layer or skimmed the top of the layer. Details of the MA over BRW and the other flights highlighted in Fig. 3b are described in Section 3.1.

Previous work that observed BrCN production from a marine diatom (*Nitzschia cf pellucida*) (Vanelslander et al., 2012) in laboratory cultures presents the possibility that the BrCN observed during ATom was emitted from marine biota. However, several aspects of the timing and location of the ATom observations argue against there being a significant biological source over most of the globe. BrCN was not observed in the marine boundary layer (MBL) over the areas of the ocean that had the highest biological productivity, as shown by the map in Fig. S3, which overlays the ATom flight tracks with the mean chlorophyll-α surface concentration as compiled by the NASA Earth Observatory (NASA, 2020). Unfortunately, this satellite product does not work over areas having significant ice cover (higher latitudes) so we cannot rule out a source from sea ice biological communities.

The CIT-CIMS Arctic winter flights from ATom-2 is the other set of observations that definitively show that BrCN is a product of abiotic Br chemistry. The two flights, Feb. 18, 2017 from the Azores to Thule, Greenland, and Feb. 19, 2017 from Thule to Anchorage, Alaska, involved low level legs over Baffin Bay, the Arctic Ocean, and MAs over BRW and the Prudhoe Bay/Deadhorse airport (SCC). There was essentially no photosynthetic activity at the Northern latitudes during this time, yet BrCN and the ratio of $CHBr_3$ to CH_2Br_2 were highly correlated (Fig. 4) and $CHBr_3/CH_2Br_2$ reached levels previously observed in the Antarctic winter (>10) (Abrahamsson et al., 2018). The data for all points in both flights imply a background in $CHBr_3/CH_2Br_2$ of 2.7 ±0.3 based on the x-intercept in Fig. 4. In these instances, there was Br activation initiated by O_3-Br^- chemistry, but no bromine explosion with the associated O_3 depletion to very low levels (<10 ppbv) as shown in Fig S4, because there was insufficient photochemistry to carry the gas phase catalytic Br chemistry. Note that ATom-1 took place during the Austral winter (August, 2016), but unlike ATom-3&4, the aircraft did not travel south of 65.3°S, no $CHBr_3/CH_2Br_2$ ratios above 2.5 were observed during that flight, and no BrCN above the CIT-CIMS detection limit was observed during the entire ATom-1 campaign.

https://doi.org/10.5194/egusphere-2023-860
Preprint. Discussion started: 30 May 2023

We examine detailed measurements from ATom-3&4 below for signs of O_3 destruction, and $CHBr_3$ and BrCN formation. These processes are in competition with one another, as they all depend HOBr/Br_2 chemistry:

305	$HOBr + Br^-_{(aq)} \rightarrow Br_2$	Bromine explosion chemistry	(R4)
	$HOBr + DOM_{(aq)} \rightarrow CHBr_3$	$CHBr_3$ formation/Active Br termination	(R5)
	$HOBr + DON_{(aq)} \rightarrow BrCN$	BrCN formation/Active Br termination	(R6)

The product channels depend on the availability of the reaction substrates: Br^-, DOM and dissolved organic nitrogen (DON), 310 and on reaction conditions (e.g., pH). As a result, we would expect some coincidence in time and space, but not necessarily close correlations between O_3 loss, excess $CHBr_3$, and the appearance of BrCN.

3.1 Case Studies

The following analysis focuses on case studies of locations within the polar boundary layer that had BrCN 315 enhancements, since BrCN was below detection limit throughout much of the troposphere. The data will be examined for: evidence of coincident BrCN appearance and O_3 destruction chemistry, co-variation of BrCN with other bromocarbons that might differentiate between biotic and abiotic origins, and indications of the processes that govern BrCN atmospheric lifetimes and removal processes. The times noted in all the following sections are Coordinated Universal Time (UTC) to maintain consistency.

320

3.1.1 October 11 and 14, 2017, May 9 2018: Southern Ocean and Weddell Sea

The first detectable BrCN during ATom-3 was found as the aircraft flew over the southern high latitudes on October 11 and 14, 2017. There was also detectable BrCN during ATom-4 on the most southerly flight on May 9, 2018, so all these flights will be considered together. The October 11, 2017 flight involved a transit over the Southern Ocean from Christchurch, 325 NZ to Punta Arenas, CL at approximately 65°S latitude. A low altitude leg at approximately 23:40 UTC descended to 172m and was over broken ice, i.e. ice with open water, as shown by the video frame in Fig. S5. The details of the BrCN and associated measurements are shown in Fig. S6, the deepest BrCN-containing layer observed during ATom-3&4. Along with the BrCN, there are slight amounts of BrCl and BrO (< 1 pptv) were detected, but O_3 was only slightly reduced (26 ppbv in the boundary layer vs 32 ppbv above), although there are not substantial amounts data to indicate what O_3 levels would be 330 expected in this environment at this time of year. HCN was depressed (50–70 pptv) in the polar boundary layer compared to the air immediately above 0.8 km altitude. The halocarbons CH_3Br and CH_3I were not elevated in the polar boundary layer leg, but $CHBr_3$ was elevated relative to CH_2Br_2, although it did not have as sharp a profile as BrCN, due to the much longer atmospheric lifetime of $CHBr_3$ relative to BrCN as discussed below. Another feature of note is that the O_3 level was quite constant (26.5 ±0.15 ppbv) in time/altitude within the intermediate polar boundary layer, which implies that if O_3 were

https://doi.org/10.5194/egusphere-2023-860
Preprint. Discussion started: 30 May 2023

destroyed due to Br chemistry in this environment it had happened sufficiently long ago that any sign of local photochemistry (e.g., in the layer closest to the surface) had mixed within at least the middle of the polar boundary layer.

The highest BrCN observed during southern hemisphere Spring was over the Weddell Sea during the Oct. 14, 2017 flight of ATom-3 at about 15:15 UTC and about 68°S latitude. This polar boundary layer leg was also over sea ice at 170 m. However, in contrast to the Oct. 11, 2017 polar boundary layer leg, this vertical profile shows that the polar boundary layer did not have a constant potential temperature even down to the lowest altitude sampled (Fig. S7). As a result, the time profiles of BrCN, and HCN, showed considerable variability at the lowest altitudes, and it is not clear from other key species, including BrCl, halocarbons and the vertical profile of O_3, how much Br-associated O_3 destruction had occurred within this polar boundary layer environment.

We observed the first firm evidence of O_3 destruction and the association of BrCN with active-Br chemistry later on the Oct. 14, 2017 flight during the polar boundary layer leg centered around 18:20 UTC ranging from 75–76°S latitude. During these vertical profiles, there was evidence of O_3 loss, and anticorrelation of O_3 and BrCN concentrations as shown in Fig. 5a&b. While it is difficult to identify a "background" O_3 level, i.e., a level of O_3 that would be present in the absence of local production or destruction or mixing down of stratospheric O_3, it seems clear from the entirety of the Oct. 14, 2017 flight that O_3 mixing ratios are in the range of 30–40 ppbv in this environment (over the Southern Ocean) at mid-tropospheric altitudes (2–6 km). During the profiles shown in Fig. 5a&3b, O_3 between 2–4 km was on the order of 32 ppbv (dashed lines in Fig. 5a&b) while O_3 at lower altitudes was sometimes below 20 ppbv and those levels were anti-correlated with BrCN. This type of profile is consistent with active-Br chemistry that involves O_3 destruction, and the production of BrCN from reactions involving active-Br compounds and reduced nitrogen substrates. In addition to this evidence, $CHBr_3$ was elevated relative to the other bromocarbons (Fig. S8) which is consistent with its abiotic production from reactions of HOBr with DOM in snow/ice and particle surfaces.

The May 9, 2018 flight during ATom-4 also flew over the Weddell Sea, this time during the Austral Fall. The BrCN mixing ratio approached 11 pptv (10 s avg), and coincided with high $CHBr_3/CH_2Br_2$ ratios (~3), but very little apparent O_3 loss (~1 ppbv). The aircraft was over the icepack, with broken leads (areas of open water where the ice pack has broken up and separated), during the two low legs where elevated BrCN was observed (14:15 UTC and 15:35 UTC) and there were substantial clouds present.

3.1.2 October 25, 2017, and May 19, 2018: Flights over the Arctic Ice Pack

The first episode in which BrCN was observed over the Arctic ice pack during ATom-3 was on the flight on Oct. 25, 2017 which was the northern-most leg from Bangor, Maine, USA to Anchorage, Alaska, USA. BrCN was elevated above the detection limit on four of the polar boundary layer legs, at levels ranging from 3.8 to 10 pptv (10s avg; Fig. S9). On each of those polar boundary layer legs, the aircraft did not reach a polar boundary layer with constant potential temperature. However, there was still some evidence for minor amounts of O_3 destruction (3–4 ppbv).

https://doi.org/10.5194/egusphere-2023-860
Preprint. Discussion started: 30 May 2023

The May 19, 2018 flight was similar to the Oct. 25, 2017 flight in that it started in Bangor and ended at Anchorage and constituted the northern most leg of ATom-4. The interesting features of this flight are that each polar boundary layer leg (aside from the final approach into Anchorage) corresponded to elevated BrCN and some degree of O_3 destruction, as shown in Fig. 6. The photochemical environment during this flight was somewhat consistent due to the fact that the aircraft was traveling east to west during daylight hours creating a situation in which the photolysis rates did not change much with time (see Fig. S10). As a result, the rates associated with Br radical chemistry (Br_2, BrCl and HOBr photolysis) were relatively consistent throughout the flight: $jBr_2 \rightarrow 2Br$ was in the range of 0.05 to 0.08 s^{-1}. The vertical profiles of potential temperature for each of the polar boundary layer legs (see Fig. S11) showed that the lowest layers had constant potential temperatures for all the legs except the one that was centered around 21:30 UTC (leg E). Each of the polar boundary layer legs during the May 19 flight displayed O_3 destruction, with the lowest O_3 on leg F averaging below 5 ppbv. Remarkably, these polar boundary layer legs displayed averages of O_3 and BrCN that were highly anti-correlated, R^2=0.94 (Fig. 7). That this anti-correlation was observed over such a wide geographic expanse could mean the that O_3 destruction chemistry was uniform (due to the relatively uniform photochemical environment). This concept is consistent with observations and analysis presented by (Jacobi et al., 2010) that indicate that O_3 destruction is widespread and persistent in the springtime Arctic boundary layer. The anti-correlation of O_3 and BrCN is a necessary, but not sufficient support for the theory that BrCN is formed by the same active-Br chemistry that destroys O_3 in the polar boundary layer. BrO and BrCl were also elevated during those low-level polar boundary layer legs (see Fig. S12), but did not anti-correlate with O_3, (R^2 = 0.11 and 0.06, respectively). The presence of those active-Br compounds means that O_3 destruction chemistry was active recently, since those compounds have lifetimes on the order of minutes to ~1hr in this environment. In contrast, current evidence implies that BrCN has a lifetime of at least 1–2 days (see Section 4.2), so its concentration will indicate integrated Br-derived O_3 destruction over time.

3.1.3 October 1, 2017 and April 27, 2018 Missed Approaches over Utqiagvik, Alaska.

The ATom-3 leg that started on Oct. 1, 2017 and flew from Palmdale, California, USA to Anchorage also included a MA over BRW at Utqiagvik shown in Fig. S13. It is instructive to examine the details of that flight as it stands in contrast to the ATom-4 MA which will be shown in detail below. This MA did not correspond to elevated BrCN concentrations; instead, the BrCN values were slightly below zero due to uncertainties in the subtraction of the instrument background during a zero, yet there is some evidence that the polar boundary layer might have experienced a moderate amount of O_3 destruction (~10–12 ppbv). One of the main differences between the Oct. 1, 2017 MA and that on Apr. 27, 2018 was the presence of low-level clouds over BRW during the Oct. 1, episode as indicated by reduced jBr_2 and confirmed by visual evidence (Fig. S14). It could be the that formation of BrCN is inhibited by the presence of clouds and/or BrCN was removed by uptake and reaction in clouds.

The last detailed episode to be explored took place on Apr. 27, 2018 during a MA over BRW, and involved the highest BrCN observed for the entire project. The aircraft got as low as 40 masl as it conducted the approach west to east over the runway that runs true east-west (see Fig. S15). The wind direction was from 100–120° and ranged from 4–14 m/s in the lowest

https://doi.org/10.5194/egusphere-2023-860
Preprint. Discussion started: 30 May 2023

2.5km of the flight path, which means that the aircraft should not have sampled recent emissions from the town of Utqiagvik, as the town is mostly north and southwest of BRW. The bottom panel of Fig. S15 is an image from the video camera on the nose of the DC-8. It shows that the ocean adjacent to Utqiagvik was packed with sea ice at least 10km out, but it is clear that further off shore there was a mixture of open water and ice. In addition, the atmosphere was relatively clear of clouds and particles. The time series of the relevant chemical measurements during this period (Fig. 8) show that BrCN was confined to the very lowest altitude of the MA. The halocarbon data showed no elevated levels of CH_2Br_2, CH_3Br and CH_3I, but significant enhancement (~×3) in $CHBr_3$ at the lowest altitude compared to the layer just above. The vertical profiles of key chemical constituents and temperature are shown in Fig. 9 for the lowest 0.6km of the MA. There is an indication of a locally-impacted layer between 0.15 and 0.3 km directly above the polar boundary layer that had elevated NO_y with an NO/NO_y ratio of ~0.5, but the lowest layer (< 0.15 km) had a constant potential temperature and had no evidence of local pollution. That lowest layer had BrCN up to 36 pptv (10s avg) and also elevated BrCl, and O_3 was as low as 32 ppbv, so reduced compared to the layer above the local pollution, which was about 45 ppbv at 0.35–0.6km.

As noted above, a general coincidence in time and place can be expected among BrCN formation, high $CHBr_3/CH_2Br_2$ ratios, and O_3 destruction because while they all depend on active-bromine chemistry, they are also in competition with each other. So, it is not surprising that the BrCN and O_3 levels from the Apr. 27, 2018 MA do not fit with the BrCN-O_3 correlation from May 19, 2018 that is shown in Fig. 7. However, the data set does show a general correspondence between the appearance of BrCN and the ratio $CHBr_3/CH_2Br_2$ as shown in Fig. 10a&b. The relationship appeared in both the Arctic and Antarctic flights but was most pronounced in the Arctic springtime. This correspondence is expected if $CHBr_3$ is formed from active bromine reacting with DOM, and BrCN from reaction with DON, as DON is a subset of DOM. We explore some of the possible relevant BrCN formation and destruction chemistry in the next section.

4 Discussion

In many of the polar boundary layer airmasses sampled, BrCN levels observed were often substantial relative to other gas phase organic bromine compounds (Br_{org}). For example, during the low altitude leg on the May 19, 2018 flight centered at 22:30, BrCN was 19 pptv while the sum of Br in $CHBr_3$, CH_2Br_2, CH_3Br, $CHBrCl_2$, and $CHBr_2Cl$ was just 16 pptv. Similarly, BrCN observed during the Apr. 27, 2018 MA, 36 pptv, was higher than the corresponding Br_{org}, 27 pptv.

The observations of BrCN in polar boundary layer air have some intriguing implications for the active Br chemistry that occurs in these environments. If there is multi-phase chemistry occurring that terminates active Br during classic “bromine explosion” chemistry to form BrCN, then the active-Br system works differently at destroying O_3 and Hg than is currently thought. This impact also depends on the fate of BrCN, which is not well understood since gas phase loss processes are either known to be, or likely to be, very slow. In addition, BrCN solubility in water is low, and its hydrolysis rates are slow at environmental pHs. Yet, circumstantial evidence (e.g., the near absence of BrCN above the polar boundary layer) indicates BrCN has a relatively short atmospheric lifetime. The mechanism for heterogenous removal of BrCN is also unclear and could

https://doi.org/10.5194/egusphere-2023-860
Preprint. Discussion started: 30 May 2023

have implications for whether that chemistry could re-form active Br, or be a net sink for active Br. We discuss the possibilities for BrCN formation chemistry and some constraints and possible mechanisms of heterogeneous loss in this section.

4.1 BrCN Formation

As noted above, formation of BrCN has been demonstrated in a number of chemical systems both abiotic and from marine biota. The bulk of the evidence in ATom-2,3&4 datasets is that BrCN formation occurs only in polar regions when there is active-Br chemistry occurring. Conversely, neither of the ATom-3&4 deployments observed instances where there was substantial O_3 destruction and no measurable BrCN present. The destruction of O_3, i.e. O_3 substantially below what is in the lowest 1–2km of the atmosphere above, is one tell-tale sign of active-Br chemistry. Another sign of active-Br chemistry is the presence of elevated $CHBr_3$ concentrations relative to the closely-related biogenic compound CH_2Br_2. These markers could be considered evidence that BrCN was produced from active-Br chemistry. As a consequence, it is useful to consider what chemistry could be forming BrCN from active Br, i.e., what is the source of reduced nitrogen and how would the heterogeneous formation chemistry work.

As with all XCN compounds, it is difficult to devise a chemical scheme in which BrCN is produced via gas-phase chemistry. There are basically two reasons for this: Br atoms are either not very reactive or only moderately reactive with most organic compounds (Barnes et al., 1989), but reasonably reactive with O_3 ($k = 1\times10^{-12}$ cm^3/molec-s). As a consequence, reaction with O_3 will out-compete any organic reactions due to its higher abundance as long as O_3 has not been completely depleted, a condition not observed in the ATom data set. Conversely, even if there were a source of CN radicals, which is quite unlikely, they react so rapidly (for example with O_2) that it is highly improbable that there could be a Br-compound that could compete with other CN reaction partners in rate or in mechanism (Manion et al., 2020).

The production of BrCN by heterogeneous or condensed phase (i.e., snow, ice, frost flower, aerosol particles) chemistry is much more plausible as condensed phase mechanisms are known. However, there are still a number of unknowns that make it difficult to construct a quantitative model. Rate constants and solubilities of the key reactants are not known in what is presumably a liquid-like layer of water below 273K. The active-Br compounds that are involved are Br_2 and HOBr, but the identity and chemistry of the N-containing substrates are uncertain. The possibilities are HCN/CN^-, and reduced N moieties (amines, amides, amino acids) that are part of DON present in polar environments. These DON compounds can be resident on particles (Dall'Osto et al., 2017) or ice/snow surfaces that are known to collect organic materials from a number of sources (McNeill et al., 2012). These include deposited atmospheric aerosol, sea spray, frost flowers, and sea water that has been wicked up into the ice floe. These sources by their nature are mostly DOM, and hence provide the substrates needed to produce $CHBr_3$ from HOBr through the haloform reaction. Thus, we would expect BrCN and $CHBr_3$ enhancements to be coincident in time and location, which is what is observed in our polar boundary layer data.

It is useful to examine whether reaction of HCN/CN^- on snow or ice to form BrCN could compete with propagation of Br-explosion chemistry through known mechanisms and how conditions, particularly substrate pH, might affect BrCN formation from that pathway. Simple calculations based on the competition of HOBr between reaction with HCN/CN^- to make

https://doi.org/10.5194/egusphere-2023-860
Preprint. Discussion started: 30 May 2023

BrCN and reaction with Br^- or Cl^- to make Br_2 or BrCl, and a box model calculation with more extensive Br chemistry(Wang and Pratt, 2017) are presented in the SI, and only summarized here. The competitive reaction analysis showed a profound pH dependence with higher BrCN formation at higher pH (Fig. S16&17). This was due to the pH dependence of HCN solubility and $HOBr/OBr^-$ equilibrium, and also pH dependences of HCN/CN^- reactions with $HOBr/OBr^-$. The box model with more extensive Br chemistry also showed a pH dependence, with higher BrCN favored at higher pH (Fig. S18), but more Br propagation at mid-range pH because of pH-independent Br chemistry in the model.

The pH of condensed phases in the Arctic environment can range from fairly acidic (pH 1–2) for aerosols (Nault et al., 2020) to over pH 8 for frost flowers or sea spray aerosol (Kalnajs and Avallone, 2006). So, the coincidence of BrCN with elevated $CHBr_3$ and O_3 depletion seen in some of the data presented here is consistent with abiotic active-Br chemistry. However, if the competition between production of BrCN and the propagation of active Br is pH dependent, we would not necessarily expect the tight anti-correlation shown in Fig. 7 for the May 19, 2018 flight, unless the conditions in which this chemistry was taking place was relatively uniform over 1000s of kilometers. Moreover, the fact that the BRW MA data do not fit with the data from the May 19, 2018 flight might simply be due to differences in amount and pH of the DON substrate available for reaction.

The observation that dihalogens are produced by photochemistry in the snowpack (Pratt et al., 2013;Custard et al., 2017;Halfacre et al., 2019) also presents the possibility that BrCN and $CHBr_3$ are produced by DON and DOM in that environment, the key reactions being with Br_2 or HOBr that are produced in the condensed phase. Since both BrCN and $CHBr_3$ are relatively insoluble they would be readily emitted to the atmosphere. Another intriguing possibility exists for the production of BrCN (and other active-Br compounds) in the snow/ice environments. The production of active Br in algae, HOBr in particular, is an enzymatic process that involves the reaction of H_2O_2 and Br^- in the presence of a peroxidase. As such, HOBr production is intimately tied to photosynthetic processes as has been shown in several laboratory studies (Hughes et al., 2013;Vanelslander et al., 2012;Moore et al., 1996). It is possible therefore, that dihalogen production, along with BrCN, and $CHBr_3$, could appear photochemical in nature, but in fact rely on the presence of photosynthetic algae, and in the case of BrCN and $CHBr_3$ the presence of DON and DOM substrates that would go along with algae in this environment. Again, the correlations of BrCN with O_3 destruction argue for a substantial source of BrCN from abiotic active-Br chemistry at least some of the time.

4.2 BrCN Loss

As described in the introduction, gas phase loss processes of BrCN are either known to be slow (photolysis lifetime ≅4 months at summer mid-latitudes) or quite likely to be slow (OH and Cl radical reaction rate constants < 10^{-14} cm^3-$molec^{-1}s^{-1}$ by analogy to HCN and CH_3CN)(Manion et al., 2020). The heterogeneous loss of BrCN to surfaces, particles or cloud water has only been estimated based on aqueous solubilities and a few liquid-phase reaction rates, e.g. hydrolysis and reaction with n-octanol(Roberts and Liu, 2019) and those range from several weeks to 0.5 years. At this point it is worth examining the ambient measurements for further indications of what the BrCN lifetime is in the polar boundary layer. Figure 11 shows

https://doi.org/10.5194/egusphere-2023-860
Preprint. Discussion started: 30 May 2023

vertical profiles of potential temperature, ozone, BrCN and the halocarbons CH_2Br_2 and $CHBr_3$ from the May 19, 2018 polar boundary layer leg at 2230 UTC that was discussed above in Section 3.1.2. There was very little BrCN above the polar boundary layer, and this was a general feature of all the instances where BrCN was observed. It is clear that BrCN shows a much sharper decrease with altitude than the bromocarbons ($CHBr_3$, CH_2Br_2) that have lifetimes on the order of 2–4 months at this latitude and season (Papanastasiou et al., 2014;Hossanini et al., 2010), thus BrCN must have a shorter lifetime than those compounds.

Most of the observations of elevated BrCN occurred within layers that had constant potential temperature and appeared relatively well-mixed, i.e. O_3 was depleted but constant. However, the interpretation of these measurements is complicated by the fact that our observations did not extend to the surface. Observations in polar boundary layers show that there are often very shallow stable layers (a few to tens of meters) close to the surface(Anderson and Neff, 2008) below a relatively well-mixed layer a few 100 meters to a kilometer in depth. This intermediate layer is usually capped by a strong temperature inversion and there are often clouds in the vicinity of the inversion. Several model studies have shown that very low diffusivities (1×10^{-3} m^2/sec) best describe atmospheric observations in and above these layers(Zeng et al., 2006;Wang et al., 2008). By analogy to molecular diffusion, this corresponds to transport times out of the boundary layer through this inversion that are quite slow (> weeks). The other factor that comes into play for many of these polar boundary layer legs is that many occurred over open leads in the ice, which are the source of vertical transport due to the effects of warmer water(Serreze et al., 1992). As a consequence, transport of BrCN out of the top of polar boundary layers is likely more limited by synoptic disturbances like frontal passage or ice lead formation. From these features we can roughly estimate that BrCN could have a lifetime as short as a day or two, but probably not longer than 10 days in the polar boundary layer, the upper limit being based roughly on the frequency of synoptic disturbances in this environment. It follows from this, and the slowness of gas phase loss processes, that heterogeneous reactions limit the BrCN atmospheric lifetime.

The rates of these possible condensed-phase reactions can be estimated in the same type of analysis employed by Roberts and Liu (2019)(Roberts and Liu, 2019), given a few assumptions about the polar boundary layers encountered in this work and Henry's Law solubilities. Deposition of a chemical species within a boundary layer can be thought of as two processes happening in series: physical transport to the surface, and chemical reaction at the surface (see for example(Cano-Ruiz et al., 1993)). These can be parameterized with a simple resistance model:

$$v_d = 1/(R_t + 1/(\gamma<c>/4)) \quad \text{(Eq1)}$$

where the total resistance is $=1/v_d$, with v_d being the deposition velocity, which can also be expressed as the mixing layer height, h, divided by the lifetime of the chemical species, in this case t_{BrCN}, and γ is the surface uptake coefficient and <c> is the mean molecular speed.

Our study lacks the detailed polar boundary layer dynamics measurements needed to fully evaluate R_t, the resistance due to turbulent diffusion in the lowest altitude legs. However, there are several aspects of the observations that allow us to make a useful limiting estimate, using the May 19, 2018 22:30 polar boundary layer leg as the prime example (Fig. 11). First,

https://doi.org/10.5194/egusphere-2023-860
Preprint. Discussion started: 30 May 2023

there were open leads (Fig. S19) that are associated with polar boundary layer mixing and relatively high mixing heights (Serreze et al., 1992;Moore et al., 2014). Second, the fact that potential temperature is constant with altitude below 300 m implies the polar boundary layer is well mixed at least as low as the aircraft sampled. Third, there were substantial vertical wind velocities measured by the gust probe aboard the DC-8 aircraft during this polar boundary layer leg, also shown in Fig. S19. All of these features support the assumption that, at least in this instance, turbulent resistance R_t is small relative to the resistance due to chemical uptake, at least in the presence of open leads. This is consistent with estimated mixing times of several hours deduced in studies of ozone and mercury in polar boundary layers impacted by open leads (Moore et al., 2014).

Consequently, if chemical uptake is the limiting loss process, we can estimate the liquid phase loss rate of BrCN (k_l) from Equations 1 and 2. The resistance due to chemical reaction is $1/(\gamma<c>/4)$ and the uptake coefficient (γ) can be estimated from the following equation assuming surface accommodation is efficient (Kolb et al., 1995)

$$\gamma = 4HRT(k_l D_a)^{1/2}/<c> \quad \text{(Eq2)}$$

where H is the Henry's coefficient, k_l is the first order liquid phase loss rate, D_a is the diffusion coefficient of the reactant in solution, and RT are the gas constant and temperature. Similarly to the analysis of HCN solubility, the parameters needed to estimate k_l will need to be extrapolated below 273K assuming the surfaces are liquid-like layers. In the case of BrCN, we use recent solubility measurements (Roberts and Liu, 2019) and assume H has the same temperature dependence (i.e., same enthalpy of solution) in the liquid-like layer below 273K. Diffusion coefficients also vary as 1/T, and although there are not measurements of D_{BrCN}, we estimate it is 0.5×10^{-5} cm^2/s at 263K by analogy to HCN and the temperature dependence of diffusion coefficients(Tyn and Calus, 1975). Thus, the first order loss rates of BrCN in solution that correspond to polar boundary layer lifetimes range from 1.2×10^{-2} s^{-1} for a lifetime of 1 day, to 1.2×10^{-4} s^{-1} for a lifetime of 10 days. This range is faster than BrCN hydrolysis, which can be extrapolated to be approximately 1.5×10^{-5} s^{-1} at 263K(Roberts and Liu, 2019). Given that any reactants other than water would be present in micromolar to nanomolar concentrations, this range of first order loss rates corresponds to second order rate constants that are in the range of 10^4–10^7 M^{-1} s^{-1}.

The possibility that BrCN could react with halide ions (Cl^-, Br^-, or I^-) and reform a dihalogen (e.g. XBr) should be considered, as those reactions would serve to propagate Br explosion chemistry. Reactions of BrCN with I^- and Br^- have been studied in solution(Nolan et al., 1975) and it was found that the rate limiting step in BrCN + I^-, which probably forms IBr, is relatively slow, 0.106 $M^{-1}s^{-1}$ at 298K. The solution-phase reaction eventually formed I_3^-, which would not be favored at typical I^- concentrations in polar environments. The reaction of BrCN with Br^- was estimated to be quite a bit slower (~10^{-8} $M^{-1}s^{-1}$) based on rate measurements of Br_2 + HCN → BrCN + Br^- + H^+, and the measured equilibrium constant:

$$K = \frac{[BrCN][H^+][Br^-]}{[HCN][Br_2]} = 6 \times 10^8 \text{ M} \quad \text{(Eq 3)}$$

https://doi.org/10.5194/egusphere-2023-860
Preprint. Discussion started: 30 May 2023

We attempted to form Br_2 in a laboratory experiment at room temperature in which saturated NaBr solution was exposed to 150 ppbv of BrCN, and no observable Br_2 resulted (upper limit of 0.1% of BrCN), consistent with the above estimate that the reaction $BrCN + Br^- \rightarrow Br_2 + CN^-$ is quite slow. Although it has not been measured to our knowledge, we can expect the reaction of BrCN with Cl^- to be quite slow as well, given established trends of halogen reactions.

The reaction of BrCN with active-halogen species, particularly HOCl or HOBr;

$$HOCl\ (or\ HOBr) + BrCN \rightarrow BrCl\ (or\ Br_2) + HOCN \quad (R4)$$

might also occur on snow/ice or particle surfaces. While there is no direct evidence for this, the addition of HOCl or Cl_2 to treated water where BrCN was present was observed to accelerate BrCN loss (Heller-Grossman et al., 1999). Such a reaction of HOCl or HOBr, combined with formation reactions discussed above would lead to no net gain or loss of active halogen to the polar boundary layer.

There are a number of other reactions that BrCN is known to undergo, aside from simple hydrolysis, but none of them generate active Br. BrCN is known to react with R-OH- or R-SH-containing compounds and substituted amines (Siddiqui and Siddiqui, 1980;Kumar, 2005), with the net reaction yielding cyanate, thiocyanate or nitrile functionalities and the Br ending up either as Br^- or as a Br-carbon compound. To our knowledge, the rate constants of these reactions have not been measured, but are likely to be reasonably fast given that many of these reactions are used for synthesis or column preparative derivatization (see for example (March et al., 1974)). The key point of emphasis here is that none of these reactions leads to the reformation of an active-Br compound.

5 Conclusions

Two different instruments measured BrCN during the NASA ATom deployments, a CF_3O^- ToF CIMS and an I^- ToF CIMS, along with two other active-bromine compounds BrCl and BrO during the NASA ATom mission deployments 3&4 in 2017 and 2018. The ATom-1&2 measurements from the CF_3O^- ToF CIMS showed that BrCN was present above detection limit (3σ of the 10 s precision = 11 pptv) only in the polar boundary layer during the Arctic winter. This Arctic BrCN approached levels as high as 38 pptv and was correlated with high ratios of $CHBr_3$-to-CH_2Br_2, a marker for active-Br chemistry in the absence of photosynthesis. The elevated BrCN and $CHBr_3$ have a common origin in the condensed-phase reactions of active bromine (HOBr, Br_2) with dissolved organic matter (DOM) and dissolved organic nitrogen (DON). In this environment, there is an absence of photochemistry, so active bromine is thought to be produced by reaction of O_3 with Br^-, and the relatively tight correlation of BrCN and $CHBr_3$/CH_2Br_2 arises due to the fact that DON is a subset of DOM.

The ATom-3&4 measurements revealed elevated mixing ratios (> 3 pptv) of BrCN in both polar boundary layers during both seasons (Spring and Fall). Mixing ratios of BrCN up to 36pptv (10s avg) were observed during a MA over BRW airport at Utqiagvik, Alaska. These observations also support the conclusion that least some of the BrCN came from active-Br

https://doi.org/10.5194/egusphere-2023-860
Preprint. Discussion started: 30 May 2023

chemistry reactions on snow, ice and particle surfaces, with the -CN group resulting from either HCN/CN^- or other reduced nitrogen species from oceanic or cryospheric sources. Instances where substantial BrCN was observed corresponded to other indicators of active-Br chemistry: O_3 depletion, elevated $CHBr_3$ relative to CH_2Br_2, and usually elevated BrO and BrCl mixing ratios. A simple competitive reaction model of the liquid phase reactions of $HOBr/OBr^-$ with HCN/CN^- or Cl^-/Br^- and a box model of Br chemistry both show that BrCN formation can compete with active-Br propagation at higher pHs (pH>6). Surface pH is a somewhat uncertain property of the liquid-like layers that are on the surfaces of aerosol, ice, and frost flowers, and it could also be that during a given O_3 depletion episode the chemistry could evolve to produce BrCN on basic surfaces such as frost flowers and brines, or as surface acidity of snow and ice is depleted.

The higher mixing ratios of BrCN observed at times during polar boundary layer legs make it a potentially important contributor to the active-Br cycle. Total inorganic Br values are typically on the order of a few tens of pptv in areas where bromine explosion chemistry is taking place (Simpson et al., 2015). In addition, very short-lived halocarbon species that contain bromine also usually amount to a few tens of pptv Br. The BrCN concentrations observed in this study were often in the same range as these important Br reservoirs.

BrCN was confined to the polar boundary layer and vertical profiles showed a sharp cut-off at the level of the temperature inversion strongly implying that BrCN has a short lifetime (1–10 days) in this environment. Given the relatively low aqueous solubility and slow hydrolysis reaction rates of BrCN, these vertical profiles imply BrCN must undergo more rapid condensed-phase reactions (10^4 –10^7 M^{-1} s^{-1}) that lead to relatively efficient uptake and loss in the polar boundary layer environment. The presence of BrCN indicates a loss of active bromine from the system since known condensed phase loss mechanisms of BrCN result in either Br^- or C-Br bonds. Preliminary laboratory experiments showed that BrCN does not reform active bromine when reacted with solution phase Br^-. Further intensive ground-based observations of BrCN with other active-Br compounds, and laboratory exploration of BrCN liquid phase reactions will lead to better characterization of the processes that control halogen-induced O_3 loss in polar regions.

6 Code availability

Statistical analyses were performed using the standard routines for averaging and ODR fitting provided by Igor Pro Version 8 software. The box model code is available on request.

7 Data availability

Data are available in the main text and supplementary materials and from the Atmospheric Tomography mission archives in the Oak Ridge National Laboratory Distributed Active Archive Center (ORNL DAAC) at https://doi.org/10.3334/ORNLDAAC/1925

https://doi.org/10.5194/egusphere-2023-860
Preprint. Discussion started: 30 May 2023

8 Supplement link

9 Author contributions

JMR wrote the paper with assistance from co-authors. JMR, PRV, JAN, MAR, JDC, and POW worked on BrCN calibration. SW performed model analyses on Br chemistry. PRV, JAN, IB, JP, TBR, CRT, HMA, JDC, POW, SRH, KU, DB, and SM conducted the ATom measurements.

10 Competing interests

The Authors declare they have no competing interests

11 Disclaimer

Mention of tradenames and brands is for information purposes only and does not imply an endorsement by the authors.

12 Acknowledgements

We thank William D. Neff and Matthew Shupe for helpful discussions. We acknowledge the ATom Science Team who contributed to this mission. We also gratefully acknowledge the NASA and ESPO project personnel who participated in this campaign. This work was supported by; The NOAA Cooperative Agreement with CIRES, NA17OAR4320101.
The ATom project, an EVS-2 Investigation under NASA Research Announcement (NRA) NNH13ZDA001N-EVS2, Research Opportunities in Space and Earth Science (ROSES-2013) and funded through NASA Agreement NNH15AB12I to NOAA.
Contributions from Caltech were funded through NASA agreements NNX15AG61A and 80NSSC21K1704.
The National Center for Atmospheric Research, which is sponsored by the National Science Foundation under Cooperative Agreement 1852977.

13 References

Abbatt, J. P. D., Thomas, J. L., K., A., Boxe, C., Granfors, A., Jones, A. E., King, M. D., Saiz-Lopez, A., Shepson, P. B., Sodeau, J., Tohhey, D. W., Toubin, C., von Glasow, R., Wren, S. N., and Yang, X.: Halogen activation via interactions with environmental ice and snow in the polar lower troposphere and other regions, Atmos. Chem. Phys., 12, 6237-6271, 10.5194/acp-12-6237-2012, 2012.
Abrahamsson, K., Granfors, A., Ahnoff, M., Cuevas, C. A., and Saiz-Lopez, A.: Organic bromine compounds produced in sea ice in Antarctic winter., Nature Commun., 9, 5291, 10.1038/s41467–018-07062-8, 2018.
Anderson, P. S., and Neff, W. D.: Boundary layer physics over snow and ice, Atmos. Chem. Phys., 8, 3563-3582, 2008.
Artiglia, L., Edebeli, J., Orlando, F., Chen, S., Lee, M.-T., Arroyo, P. C., Gilgen, A., Bartels-Rausch, T., Kleibert, A., Vazdar, M., Carignano, M. A., Francisco, J. S., Shepson, P. B., Gladich, I., and Ammann, M.: A surface-stabilized

https://doi.org/10.5194/egusphere-2023-860
Preprint. Discussion started: 30 May 2023

ozonide triggers bromide oxidation at the aqueous solution-vapour interface, Nature Commun., 8, 700, 10.1038/s41467-017-00823-x, 2017.

Barnes, I., Bastian, V., Becker, K. H., Overath, R., and Zhu, T.: Rate constants for the reactions of Br atoms with a series of alkanes, alkenes, and alkynes in the presence of O_2., Int. J. Chem. Kinet., 21, 499-517, 10.1002/kin.550210703, 1989.

Barrie, L. A., Bottenheim, J. W., Schnell, R. C., Crutzen, P. J., and Rasmussen, R. A.: Ozone destruction and photochemical reactions at polar sunrise in the lower Arctic atmosphere, Nature, 334, 138-141, 10.1038/334138a0, 1988.

Bourgeois, I., Peischl, J., Neuman, J. A., Brown, S. S., Thompson, C. R., Aikin, K. C., Allen, H. M., Angot, H., Apel, E. C., Baublitz, C. B., Brewer, J. F., Campuzano-Jost, P., Commane, R., Crounse, J. D., Daube, B. C., DiGangi, J. P., Diskin, G. S., Emmons, L. K., Fiore, A. M., Gzatzelis, G. I., Hills, A., Hornbrook, R. S., Huey, L. G., Jimenez, J. L., Kim, M., Lacey, F., McKain, K., Murray, L. T., Nault, B. A., Parrish, D. D., Ray, E., Sweeney, C., Tanner, D. J., Wofsy, S. C., and Ryerson, T. B.: Large contribution of biomass burning emissions to ozone throughout the global remote troposphere, Proc Natl Acad Sci., 118, e2109628118, 2021.

Cano-Ruiz, J. A., Kong, D., Balas, R. B., and Nazaroff, W. W.: Removal of reactive gases at indoor surfaces: Combining mass transport and surface kinetics Atmos. Environ., 27A, 2039-2050, 1993.

Carpenter, L. J., Hopkins, J. R., Jones, C. E., Lewis, A. C., Parthipan, R., Wevill, D. J., Poissant, L., Pilote, M., and Constant, P.: Abiotic source of reactive organic halogens in the sub-Arctic atmosphere?, Environ. Sci. Technol., 39, 8812-8816, 10.1021/es050918w, 2005.

Clifford, D., and Donaldson, D. J.: Direct experimental evidence for a heterogeneous reaction of ozone with bromide at the air−aqueous interface, J. Phys. Chem. A, 111, 9809-9814, 10.1021/jp074315d, 2007.

Custard, K. D., Raso, A. R. W., Shepson, P. B., Staebler, R. M., and Pratt, K. A.: Production and release of molecular bromine and chlorine from the Arctic coastal snowpack, ACS Earth Space Chem., 1, 142-151, 10.1021/acsearthspacechem.7b00014, 2017.

Daiber, E. J., DeMarini, D. M., Ravuri, S. A., Liberatore, H. K., Cuthbertson, A. A., Thompson-Klemish, A., Byer, J. D., Schmid, J. E., Afifi, M. Z., Blatchley II, E. R., and Richardson, S. D.: Progressive increase in disinfection byproducts and mutagenicity from source to tap to swimming pool and spa water: Impact of human inputs, Environ. Sci. Technol., 50, 6652-6662, 10.1021/acs.est.6b00808, 2016.

Dall'Osto, M., Ovadnevaite, J., Paglione, M., Beddows, D. C. S., Ceburnis, D., Cree, C., Cortés, P., Zamanillo, M., Nunes, S. O., Pérez, G. L., Ortega-Retuerta, Emelianov, M., Vaqué, D., Marrasé, C., Estrada, M., Sala, M. M., Fitzsimons, M. F., Beale, R., Airs, R., Rinaldi, M., Decessari, S., Facchini, M. C., Harrison, R. M., O'Dowd, C., and Simo, R.: Antarctic sea ice region as a source of biogenic organic nitrogen in aerosols, Scientific Reports, 7, 6047, 10.1038/s41598-017-06188-x, 2017.

Gilman, J. B., Burkhart, J. F., Lerner, B. M., Williams, E. J., Kuster, W. C., Goldan, P. D., Murphy, P. C., Warneke, C., Fowler, C., Montzka, S. A., Miller, B. R., Miller, L., Oltmans, S. J., Ryerson, T. B., Cooper, O. R., Stohl, A., and de Gouw, J. A.: Ozone variability and halogen oxidation within the Arctic and sub-Arctic springtime boundary layer., Atmos. Chem. Phys., 10, 10223-10236, 10.5194/acp-10-10223-2010, 2010.

Halfacre, J. W., Shepson, P. B., and Pratt, K. A.: pH-Dependent production of molecular chlorine, bromine, and iodine from frozen saline surfaces, Atmos. Chem. Phys., 19, 4917-4931, 10.5194/acp-19-4917-2019, 2019.

Hall, S. R., Ullmann, K., Prther, M. J., Flynn, C. M., Murray, L. T., Fiore, A. M., Correa, G., Strode, S. A., Steenrod, S. D., Lamarque, J.-F., Guth, J., Josse, B., Flemming, J., Huijen, V., Abraham, N. L., and Archibald, A. T.: Cloud impacts on photochemistry: Building a climatology of photolysis rates from the Atmospheric Tomography mission, Atmos. Chem. Phys., 18, 16809-16828, 10.5194/acp-18-16809-2018, 2018.

Heller-Grossman, L., Idin, A., Limoni-Relis, B., and Rebhun, M.: Formation of cyanogen bromide and other volatile DBPs in the disinfection of bromide-rich lake water, Environ. Sci. Technol., 33, 932-937, 10.1021/es980147e, 1999.

Hossanini, R., Chipperfield, M. P., Monge-Sanz, B. M., Richards, N. A. D., Atlas, E., and Blake, D. R.: Bromoform and dibromomethane in the tropics: a 3-D model study of chemistry and transport, Atmos. Chem. Phys., 10, 719-735, 2010.

Hughes, C., Johnson, M., Utting, R., Turner, S., Malin, G., Clarke, A., and Liss, P. S.: Microbial control of bromocarbon concentrations in coastal waters of the western Antarctic Peninsula, Marine Chem., 151, 35-46, 10.1016/j.marchem.2013.01.007, 2013.

https://doi.org/10.5194/egusphere-2023-860
Preprint. Discussion started: 30 May 2023

Jacobi, H.-W., Morin, S., and Bottenheim, J. W.: Observation of widespread depletion of ozone in the springtime boundary layer of the central Arctic linked to mesoscale synoptic conditions, J. Geophys. Res. Atmos., 115, D17302, 10.1029/2010JD013940, 2010.

Kalnajs, L. E., and Avallone, L. M.: Frost flower influence on springtime boundary-layer ozone depletion events and atmospheric bromine levels, Geophys. Res. lett., 33, L10810, 10.1029/2006GL025809, 2006.

Kolb, C. E., Worsnop, D. R., Zahniser, M. S., Davidovits, P., Keyser, L. F., Leu, M.-T., Molina, M. J., Hanson, D. R., Ravishankara, A. R., Williams, L. R., and Tolbert, M. A.: Laboratory studies of atmospheric heterogeneous chemistry, in: Progress and Problems in Atmospheric Chemistry, edited by: Barker, J. R., Advanced Series in Physical Chemistry, 3, World Scientific, Singapore, 771-875, 1995.

Kumar, V.: Cyanogen Bromide (CNBr), Synlett, 10, 1638-1639, 10.1055/s-2005-869872;, 2005.

Liu, X., Deming, B., Pagonis, D., Day, D. A., Palm, B. B., Talukdar, R., Roberts, J. M., Veres, P. R., Krechmer, J., Thornton, J. A., de Gouw, J. A., Ziemann, P. J., and Jimenez, J. L.: Effects of gas-wall interactions on measurements of semivolatile compounds and small polar molecules, Atmos. Meas. Tech., 12, 3137-3149, 10.5194/amt-12-3137-2019, 2019.

Maas, J., Tegtmeier, S., Quack, B., Biastoch, A., Durgadoo, J. V., Ruhs, S., Gollasch, S., and David, M.: Simulating the spread of disinfection by-products and anthropogenic bromoform emissions from ballast water discharge in Southeast Asia, Ocean Sci., 15, 891-904, 10.5194/os-15-891-2019, 2019.

Madronich, S., and Flocke, S.: The Role of Solar Radiation in Atmospheric Chemistry, in: Environmental Photochemistry, The Handbook of Environmental Chemistry (Reactions and Processes), edited by: Boule, P., Springer, Heidelberg, 1999.

NIST Chemical Kinetics Database, NIST Standard Reference Database 17, Version 7.0 (Web Version), Release 1.6.8, Data version 2015.09, https://kinetics.nist.gov/, 2020.

March, S. C., Parikh, I., and Cuatrecasas, P.: A simplified method for cyanogen bromide activation of agarose for affinity chromatography, Anal. Biochem., 60, 149-152, 10.1016/0003-2697(74)90139-0, 1974.

Mattila, J. M., Arata, C., Wang, C., Katz, E. F., Abeleira, A., Zhou, Y., Zhou, S., Goldstein, A. H., Abbatt, J. P. D., DeCarlo, P. F., and Farmer, D. K.: Dark chemistry during bleach cleaning enhances oxidation of organics and secondary organic aerosol production indoors, Environ. Sci. Technol. Lett., 7, 795-801, 10.1021/acs.estlett.0c00573, 2020.

McNeill, V. F., Grannas, A. M., Abbatt, J. P. D., Ammann, M., Ariya, P., Bartels-Rausch, T., Domine, F., Donaldson, D. J., Guzman, M. I., Heger, D., Kahan, T. F., Klan, P., Masclin, S., Toubin, C., and Voisin, D.: Organics in environmental ices: sources, chemistry, and impacts, Atmos. Chem. Phys., 12, 9653-9678, 10.5194/acp-12-9653-2012, 2012.

Mehlmann, M., Quack, B., Atlas, E., Hepach, H., and Tegtmeier, S.: Natural and anthropogenic sources of bromoform and dibromomethane in the oceanographic and biogeochemical regime of the subtropical North East Atlantic, Environ. Sci. Processes, 22, 679-707, 10.1039/c9em00599d, 2020.

Moore, C. W., Obrist, D., Steffen, A., Staebler, R. M., Douglas, T. A., Richter, A., and Ngheim, S. V.: Convective forcing of mercury and ozone in the Arctic boundary layer induced by leads in sea ice, Nature, 506, 81-84, 10.1038/nature12924, 2014.

Moore, R. M., Webb, M., Tokarczyk, R., and Wever, R.: Bromoperoxidase and iodoperoxidase enzymes and production of halogenated methanes in marine diatom cultures, J. Geophys. Res. C, 101, 20899-20908, 10.1029/96JC01248, 1996.

NASA Earth Observations: https://neo.sci.gsfc.nasa.gov/view.php?datasetId=MY1DMM_CHLORA&year=2018, 2020.

Nault, B. A., Campuzano-Jost, P., Day, D. A., Guo, H., Jo, D., Handschy, A., Pagonis, D., Schroder, J. C., Schueneman, M., Cubison, M. J., Dibb, J. E., Hodzic, A., Hu, W., Palm, B. B., and Jimenez, J. L.: Interferences with aerosol acidity quantification due to gas-phase ammonia uptake onto acidic sulfate filter samples, Atmos. Meas. Technol., 13, 6193-6213, 0.5194/amt-13-6193-2020, 2020.

Neuman, J. A., Nowak, J. B., Huey, L. G., Burkholder, J. B., Dibb, J. E., Holloway, J. S., Liao, J., Peischl, J., Roberts, J. M., Ryerson, T. B., Scheuer, E., Stark, H., Stickel, R. E., Tanner, D. J., and Weinheimer, A.: Bromine measurements in ozone depleted air over the Arctic Ocean, Atmos. Chem. Phys., 10, 6503-6514, 10.5194/acp-10-6503-2010, 2010.

Nolan, M. F., Pendelbury, J. N., and Smith, R. H.: Kinetics of the reactions Br_2 + HCN, BrCN + I^-, $S(CN)_2$, + I^- in aqueous acid solution, Int. J. Chem. Kinet., 7, 205-214, 10.1002/kin.550070205, 1975.

https://doi.org/10.5194/egusphere-2023-860
Preprint. Discussion started: 30 May 2023

Osthoff, H. D., Roberts, J. M., Ravishankara, A. R., Williams, E., Lerner, B. M., Sommariva, R., Bates, T. S., Coffman, D., Quinn, P. K., Dibb, J. E., Stark, H., Burkholder, J. B., Talukdar, R. K., Meagher, J., Fehsenfeld, F. C., and Brown, S. S.: High levels of nitryl chloride in the polluted subtropical marine boundary layer, Supplementary Information, Nature Geoscience, 1, 324-328, 2008.

Oum, K. W., Lakin, M. J., and Finalyson-Pitts, B. J.: Bromine activation in the troposphere by the dark reaction of O_3 with seawater ice, Geophys. Res. Lett., 25, 3923-3926, 10.1029/1998GL900078, 1998.

Papanastasiou, D. K., McKeen, S. A., and Burkholder, J. B.: The very short-lived ozone depleting substance $CHBr_3$ (bromoform): revised UV absorption spectrum, atmospheric lifetime and ozone depletion potential, Atmos. Chem. Phys., 14, 3017-3025, 10.5194/acp-14-3017-2014, 2014.

Platt, U., and Janssen, C.: Observation and role of the free radicals NO_3, ClO, BrO and IO in the troposphere, Faraday Discuss., 100, 175-198, 10.1039/FD9950000175, 1995.

Pratt, K. A., K.D., C., Shepson, P. B., Douglas, T. A., Pohler, D., General, S., Zielcke, J., Simpson, W. R., Platt, U., D.J., T., Huey, L. G., Carlsen, M., and Stirm, B. H.: Photochemical production of molecular bromine in Arctic surface snowpacks, Nature Geosci., 6, 351-356, 10.1038/NGEO1779, 2013.

Roberts, J. M., and Liu, Y.: Solubility and solution-phase chemistry of isocyanic acid, methyl isocyanate and cyanogen halides, Atmos. Chem. Phys., 19, 4419-4437., 2019.

Robinson, M. A., Neuman, J. A., Huey, L. G., Roberts, J. M., Brown, S. S., and Veres, P. R.: Temperature dependent sensitivity of iodide chemical ionization mass spectrometers, Atmos. Meas. Tech. Discuss., 10.5194/amt-2022-295, 2022.

Sakamoto, Y., Goda, M., and Hirokawa, J.: Kinetics study of heterogeneous bromine release from the reaction between gaseous ozone and aqueous bromide solution, J. Phys. Chem. A, 122, 2723-2731, 10.1021/acs.jpca.7b12819, 2018.

Schlorke, D., Flemming, J., Birkemeyer, C., and Arnhold, J.: Formation of cyanogen iodide by lactoperoxidase, J. inorg. Biochem., 154, 35-41, 10.1016/j.jinorgbio.2015.11.005, 2016.

Serreze, M. C., Maslanik, J. A., Rehder, M. C., Schnell, R. C., Kahl, J. D., and Andreas, E. L.: Theoretical heights of buoyant convection above open leads in the winter Arctic pack ice cover, J. Geophys. Res. Oceans, 97, 9411-9422, 10.1029/92JC00688, 1992.

Shah, A. D., and Mitch, W. A.: Halonitroalkanes, halonitriles, haloamides, and N-nitrosamines: A critical review of nitrogenous disinfection byproduct formation pathways, Environ. Sci. Technol., 46, 119-131, 10.1021/es203312s, 2012.

Siddiqui, S., and Siddiqui, B. S.: Some extensions of von braun (BrCN) reaction on organic bases, Z. Naturforsch., 35b, 1049-1052, 1980.

Simpson, I. J., Blake, D. R., Blake, N. J., Meinardi, S., Barletta, B., Hughes, S. C., Fleming, L. T., Crawford, J. H., Diskin, G. S., Emmons, L. K., Fried, A., Guo, H., Peterson, D. A., Wisthaler, A., Woo, J.-H., Barre, J., Gaubert, B., Kim, J., Kim, M. J., Kim, Y., Knote, C., Mikoviny, T., Pusede, S. E., Schroeder, J. R., Wang, Y., Wennberg, P. O., and Zeng, L.: Characterization, sources and reactivity of volatile organic compounds (VOCs) in Seoul and surrounding regions during KORUS-AQ, Elementa, 8, 37, doi.org/10.1525/elementa.434, 2020.

Simpson, W. R., von Glasow, R., Riedel, K., Anderson, P., Ariya, P., Burrows, J., Carpenter, L. J., FrieB, U., Goodsite, M. E., Heard, D., Hutterli, M., Jacobi, H.-W., Kaleschke, L., Neff, B., Plane, J., Platt, U., Richter, A., Roscoe, H., Sander, R., Shepson, P., Sodeau, J., Steffen, A., Wagner, T., and Wolff, E.: Halogens and their role in polar boundary-layer ozone depletion, Atmos. Chem. Phys., 7, 4375-4418, 2007.

Simpson, W. R., Brown, S. S., Saiz-Lopez, A., Thornton, J. A., and von Glasow, R.: Tropospheric halogen chemistry: Sources, cycling, and impacts, Chem Rev., 115, 4035-4062, 10.1021/cr5006638, 2015.

Stockwell, C. E., Kupc, A., Witkowski, B., Talukdar, R. K., Liu, Y., Selimovic, V., Zarzana, K. J., Sekimoto, K., Warneke, C., Washenfelder, R. A., Yokelson, R. J., Middlebrook, A. M., and Roberts, J. M.: Characterization of a catalyst-based conversion technique to measure total particle nitrogen and organic carbon and comparison to a particle mass measurement instrument, Atmos. Meas. Tech., 11, 2749-2768, 2018.

Thompson, C. R., Wofsy, S. C., Prather, M. J., Newman, P. A., Hanisco, T. F., Ryerson, T. B., Fahey, D. W., Apel, E. C., Brock, C. A., Brune, W. H., Froyd, K., Katich, J. M., Nicely, J. M., Peischl, J., Ray, E., Veres, P. R., Wang, S., Allen, H. M., Asher, E., Bian, H., Blake, D., Bourgeois, I., Budney, J., Bui, T. P., Butler, A., Campuzano-Jost, P., Chang, C., Chin, M., Commane, R., Correa, G., Crounse, J. D., Daube, B., Dibb, J. E., DiGangi, J. P., Diskin, G. S.,

https://doi.org/10.5194/egusphere-2023-860
Preprint. Discussion started: 30 May 2023

Dollner, M., Elkins, J. W., Fiore, A. M., Flynn, C. M., Guo, H., Hall, S. R., Hannun, R. A., Hills, A., Hintsa, E. J., Hodzic, A., Hornbrook, R. S., Huey, L. G., Jimenez, J. L., Keeling, R. F., Kim, M. J., Kupc, A., Lacey, F., Lait, L. R., Lamarque, J.-F., Liu, J., McKain, K., Meinardi, S., Miller, D. O., Montzka, S. A., Moore, F. L., Morgan, E. J., Murphy, D. M., Murray, L. T., Nault, B. A., Neuman, J. A., Nguyen, L., Gonzalez, Y., Rollins, A., Rosenlof, K., Sargent, M., Schill, G., Schwarz, J. P., Clair, J. M. S., Steenrod, S. D., Stephens, B. B., Strahan, S. E., Strode, S. A., Sweeney, C., Thames, A. B., Ullmann, K., Wagner, N., Weber, R., Weinzierl, B., Wennberg, P. O., Williamson, C. J., Wolfe, G. M., and Zeng, L.: The NASA Atmospheric Tomography (ATom) Mission: Imaging the chemistry of the global atmosphere, Bulletin of the American Meteorological Society, 103, E761-E790, 10.1175/bams-d-20-0315.1, 2022.

Tyn, M. T., and Calus, W. F.: Diffusion coefficients in dilute binary liquid mixtures, J. Chem Eng Data, 20, 106-109, 10.1021/je60064a006, 1975.

Vanelslander, B., Paul, C., Grueneberg, J., Prince, E. K., Gillard, J., Sabbe, K., Pohnert, G., and Vyeverman, W.: Daily bursts of biogenic cyanogen bromide (BrCN) control biofilm formation around a marine benthic diatom., Proc. Natl Acad. Sci., 109, 2412-2417, doi/10.1073/pnas.1108062109, 2012.

Veres, P. R., Neuman, J. A., Bertram, T. H., Assaf, E., Wolfe, G. M., WIlliamson, C. J., Weinzierl, B., Tilmes, S., Thompson, C. R., Thames, A. B., Schroder, J. C., Saiz-Lopez, A., Rollins, A. W., Roberts, J. M., Price, D., Peischl, J., Nault, B. A., Møller, K. H., MIller, D. O., Meinardi, S., Li, Q., Lamarque, J.-F., Kupc, A., Kjaergaard, H. G., Kinnison, D., Jimenez, J. L., Jernigan, C. M., Hornbrook, R. S., Hills, A., Dollner, M., Day, D. A., Cuevas, C. A., Campuzano-Jost, P., Burkholder, J. B., Bui, T. P., Brune, W. H., Brown, S. S., Brock, C. A., Bourgeois, I., Blake, D. R., Apel, E. C., and Ryerson, T. B.: Global airborne sampling reveals a previously unobserved dimethyl sulfide oxidation mechanism in the marine atmosphere, Proc. Natl Acad. Sci., 117, 4505-4510, 10.1073/pnas.1919344117, 2020.

Wang, S., and Pratt, K. A.: Molecular halogens above the Arctic snowpack: Emissions, diurnal variations, and recycling mechanisms, J. Geophys. Res. Atmos., 122, 11,991-912,007, 10.1002/2017JD027175, 2017.

Wang, Y., Choi, Y., Zeng, T., Davis, D., Buhr, M., Huey, G., and Neff, W. D.: Assessing the photochemical impact of snow NOx emissions over Antarctica during ANTCI 2003. , Atmso. Environ., 41, 3944-3958, 10.1016/j.atmosenv.2007.07.062, 2008.

Wennberg, P.: Bromine explosion, Nature, 397, 299-301, 1999.

Wurtz, A.: Untersuchungen uber das chlorcyan, Justus Liebigs Annalen der Chemie, 79, 280-289, 1851.

Yang, X., and Shang, C.: Chlorination byproduct formation in the presence of humic acid, model nitrogenous organic compounds, ammonia, and bromide, Environ. Sci. Technol., 38, 4995-5001, 10.1021/es049580g, 2004.

Zeng, T., Wang, Y., Chance, K., Blake, N., Blake, D., and Ridley, B.: Halogen-driven low-altitude O_3 and hydrocarbon losses in spring at northern high latitudes, J. Geophys. Res. Atmos., 111, D17313, 10.1029/2005JD006706, 2006.

Zgliczynski, J. M., and Stelmaszynska, T.: Hydrogen cyanide and cyanogen chloride formation by the myeloperoxidase-H_2O_2-Cl^- system, Biochimica et Biophysica (BBA)-Enzymology, 567, 309-314, 10.1016/0005-2744(79)90116-5, 1979.

https://doi.org/10.5194/egusphere-2023-860
Preprint. Discussion started: 30 May 2023

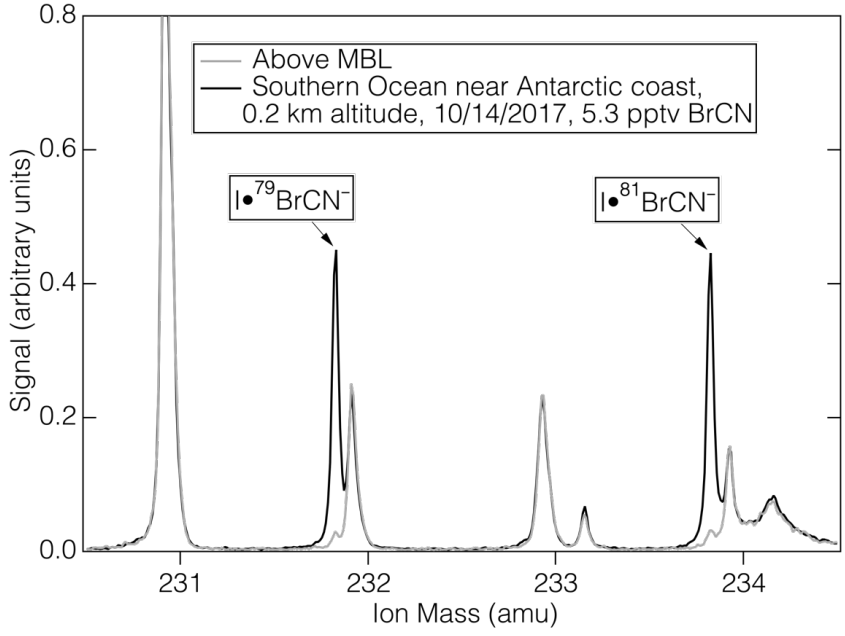

Figure 1: The mass spectra of ambient air (1 s average) during sampling in the marine boundary layer near Antarctica (black) and that of ambient air above the MBL (grey).

850

https://doi.org/10.5194/egusphere-2023-860
Preprint. Discussion started: 30 May 2023

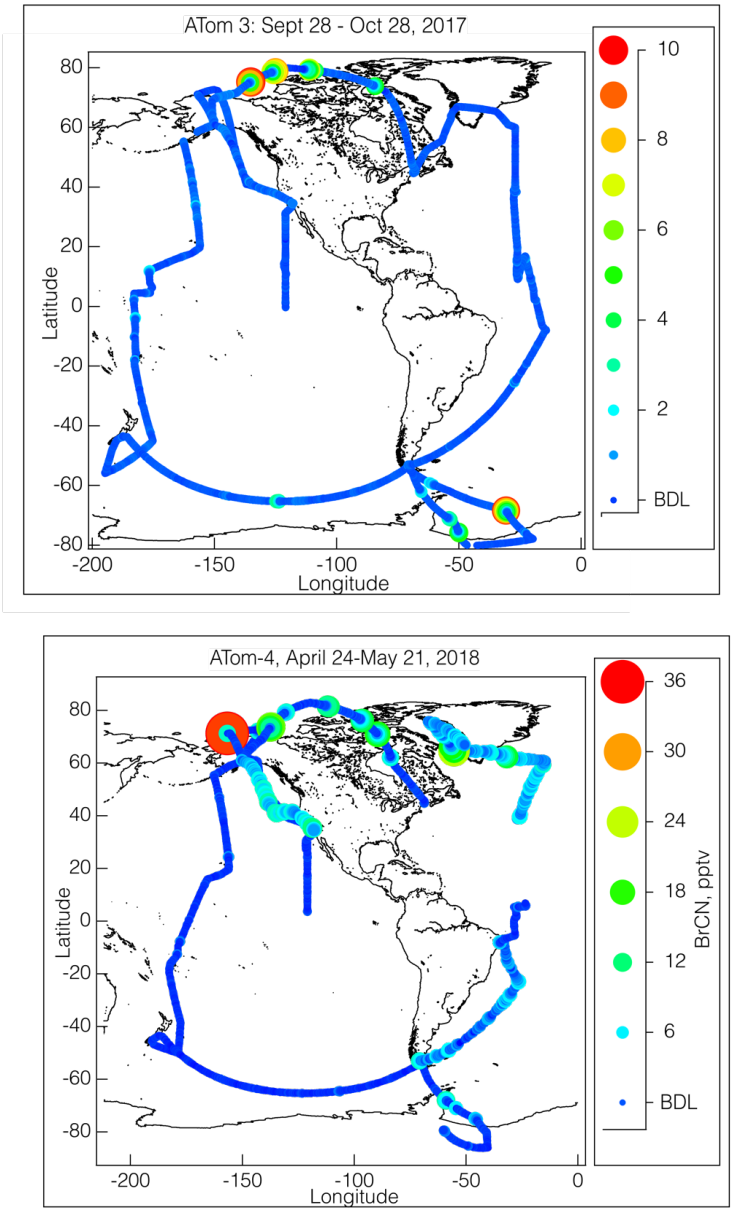

Figure 2. Maps of the BrCN mixing ratios (10s averages) observed during ATom-3 (top panel) and ATom-4 (bottom panel) colored and sized by mixing ratio, as shown by the adjacent scales.

https://doi.org/10.5194/egusphere-2023-860
Preprint. Discussion started: 30 May 2023

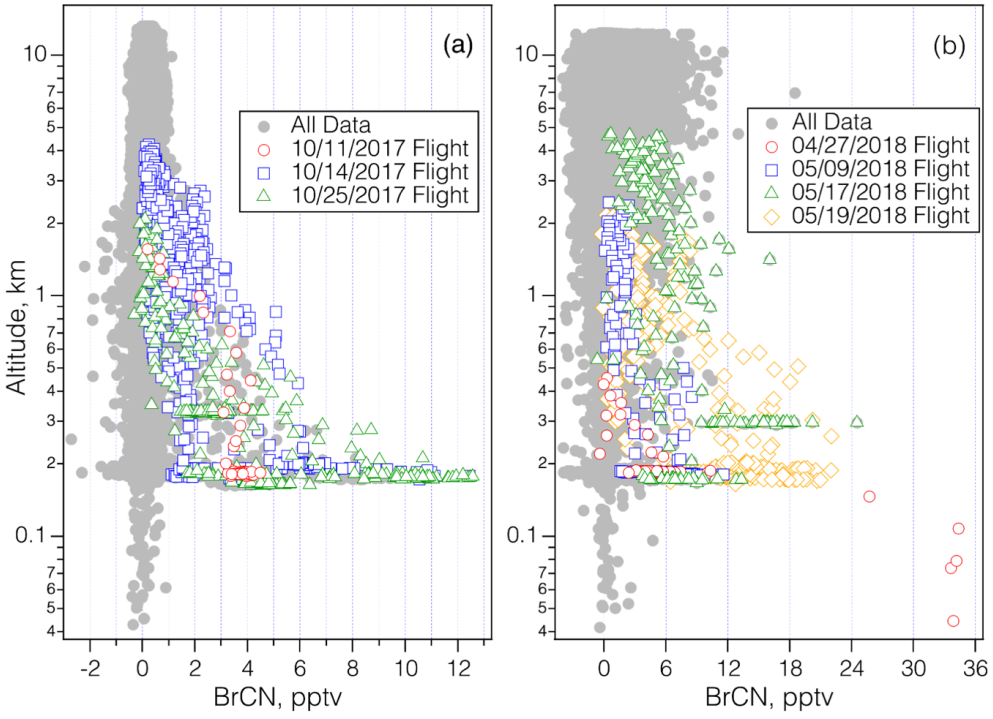

860 **Figure 3. Vertical profiles of BrCN mixing ratios (10 s averages) measured during ATom-3 (panel a) and ATom-4 (panel b). The colored points correspond to the lowest 4 km of altitude profiles that encompassed polar boundary layer dips on dates noted when enhanced BrCN was observed, and the grey points show the remaining observations.**

https://doi.org/10.5194/egusphere-2023-860
Preprint. Discussion started: 30 May 2023

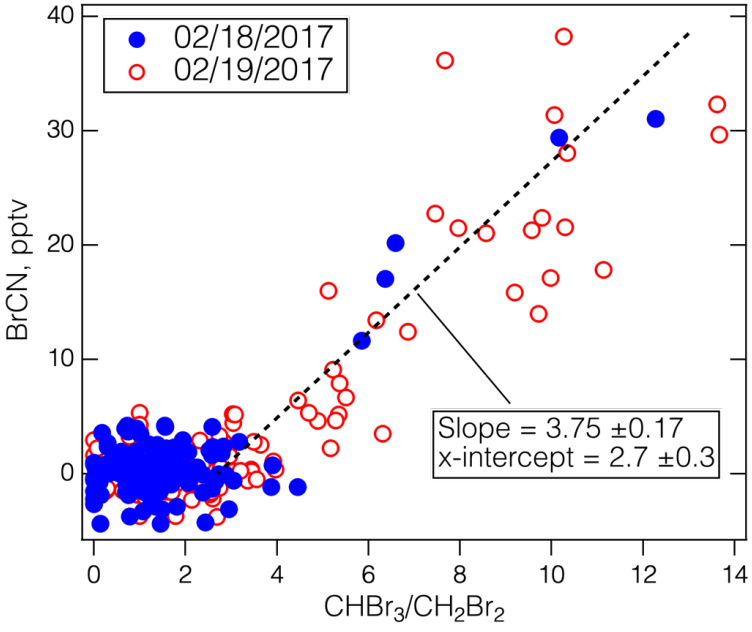

865

Figure 4. The BrCN observed by the CIT-CIMS during the ATom-2 Arctic flights versus the ratio $CHBr_3/CH_2Br_2$ measured by the UCI-WAS. The CIT-CIMS data were averaged over the UCI-WAS sample collection times. The blue points are from the Feb. 18,2017 flight from the Azores to Thule, Greenland, and the red circles are from the Feb. 19, 2017 flight from Thule to Anchorage, Alaska. The dashed line is an iterative fit assuming a background in $CHBr_3/CH_2Br_2$ and using ODR.

https://doi.org/10.5194/egusphere-2023-860
Preprint. Discussion started: 30 May 2023

870

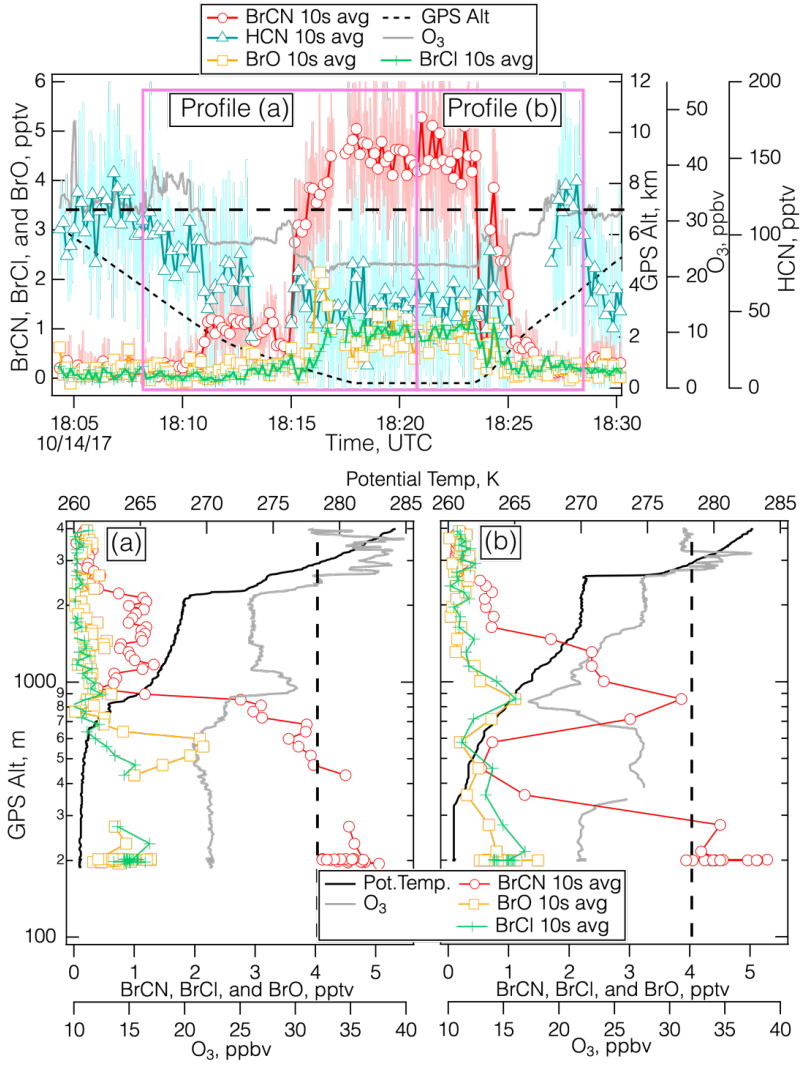

Figure 5. Details of the measurements during the polar boundary layer leg of the Oct. 14, 2017 flight over the Weddell Sea centered around 18:20 UTC. The top panel shows the time series for BrCN, BrO, BrCl, HCN, O_3, and altitude, divided into vertical profiles during the descent (Panel a), and the ascent (Panel b), and a dashed line drawn at 32 ppbv O_3.

875

https://doi.org/10.5194/egusphere-2023-860
Preprint. Discussion started: 30 May 2023

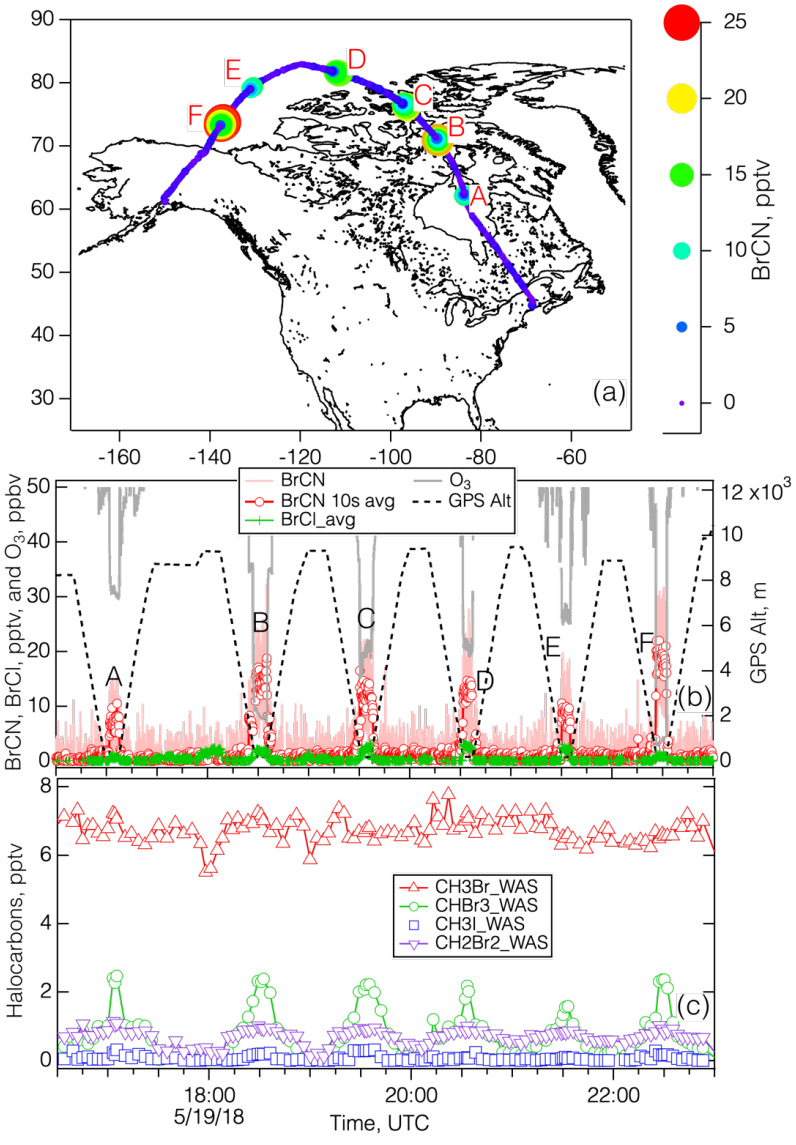

Figure 6. Panel (a) shows the map of the May 19, 2018 flight during ATom-4, with the flightpath colored and sized by BrCN, and the polar boundary layer legs labeled A–F. Panel (b) shows the time series of measured BrCN, BrCl and O_3 and the associated altitude and polar boundary layer leg. Panel (c) shows selected halocarbons measured by whole air sampling during the flight.

880

https://doi.org/10.5194/egusphere-2023-860
Preprint. Discussion started: 30 May 2023

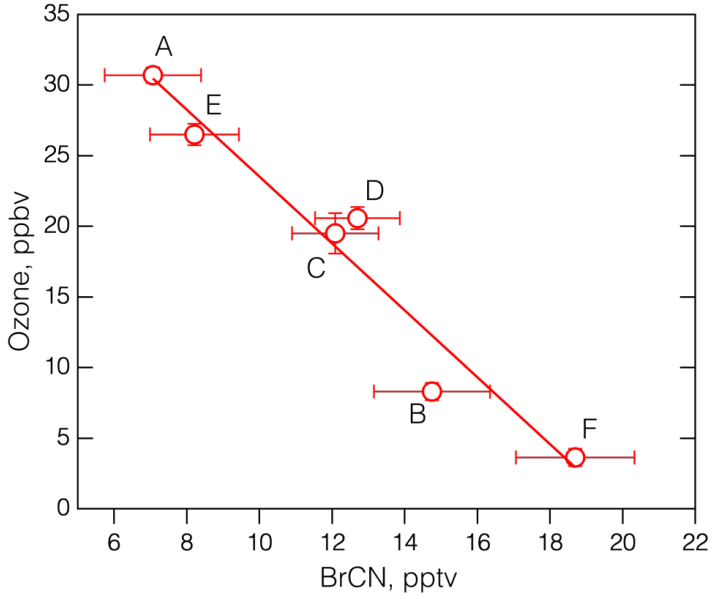

Figure 7. The average O_3 vs. the average BrCN measured during the polar boundary layer legs of the May 19, 2018 flight of ATom-4. The bars denote the standard deviation of the means and the labels correspond to the periods shown in Figure 5b. The linear regression line drawn through the points has an $R^2 = 0.94$.

https://doi.org/10.5194/egusphere-2023-860
Preprint. Discussion started: 30 May 2023

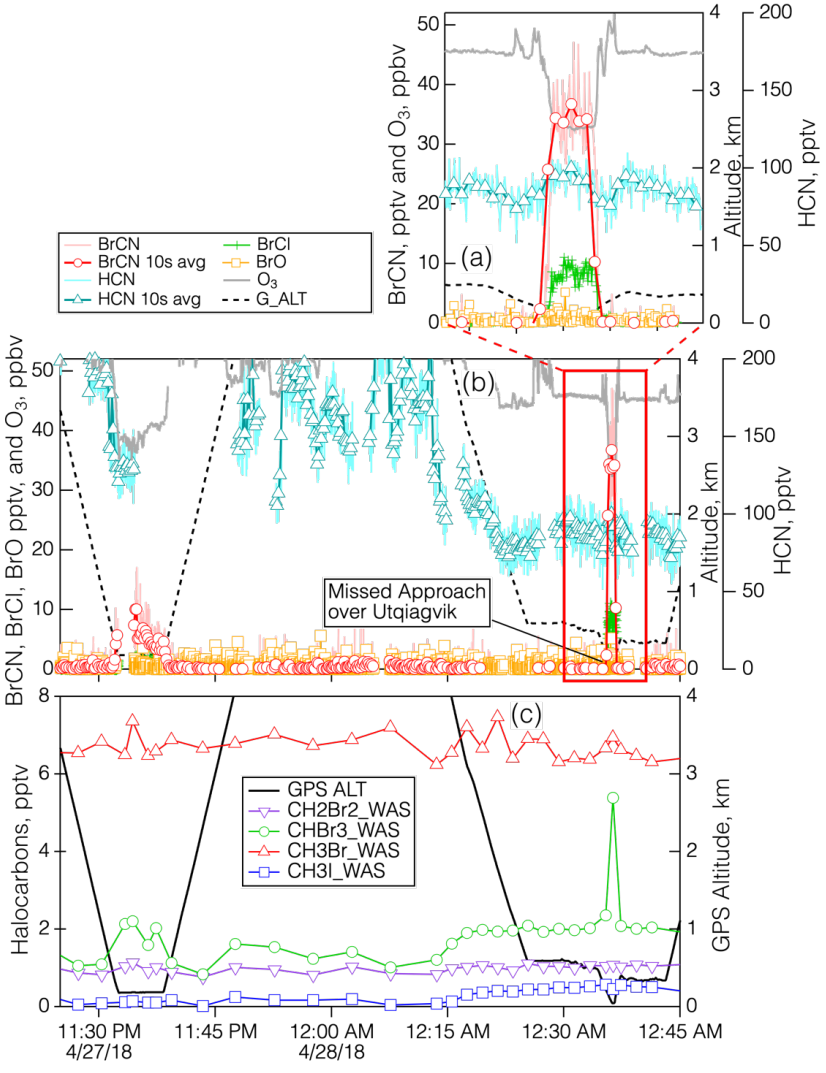

885

Figure 8. Details of the measurements during the polar boundary layer legs of the Apr. 27, 2018 flight when the aircraft executed a MA over BRW. Panel (b) shows the time series for BrCN, BrCl, BrO, HCN, O_3, and altitude, and Panel (a) shows the same time series expanded to show the lowest altitudes in more detail. Panel (c) shows the time series of the halocarbons CH_3Br, CH_3I, CH_2Br_2, and $CHBr_3$. The duration of the WAS samples was shorter than the width of the symbols.

890

https://doi.org/10.5194/egusphere-2023-860
Preprint. Discussion started: 30 May 2023

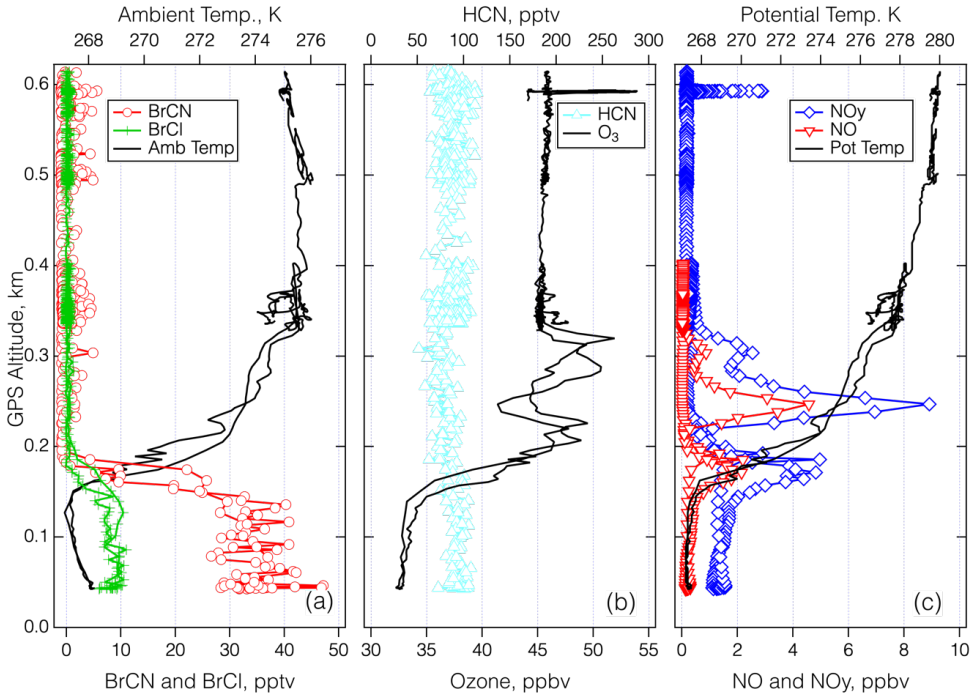

Figure 9. Vertical profiles over BRW on Apr. 27–28, 2018 for the period between 00:25 and 00:43 UTC. Panel (a) shows the 1s measurements of BrCN, BCl, and ambient temperature. Panel (b) shows 1s measurements of HCN and O_3, and Panel (c) shows 1s measurements of NOy, NO and potential temperature.

https://doi.org/10.5194/egusphere-2023-860
Preprint. Discussion started: 30 May 2023

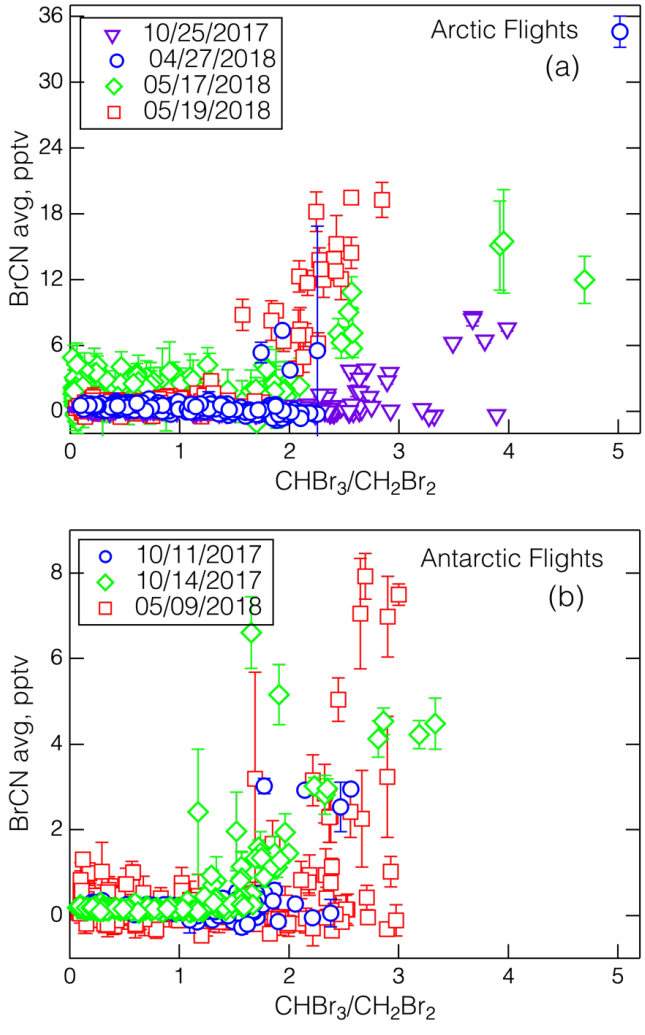

Figure 10. The relationships between BrCN (10 s data averaged over the start and stop times of the WAS) and the ratio $CHBr_3/CH_2Br_2$ for the Arctic legs (panel a) and Antarctic legs (panel b), with the corresponding dates as noted, with the standard deviation of the averages shown as error bars. Note the May 09, 2018 and May 17, 2018 data show the effects of degraded sensitivity due to the altered IMR humidity uses on those flights.

https://doi.org/10.5194/egusphere-2023-860
Preprint. Discussion started: 30 May 2023

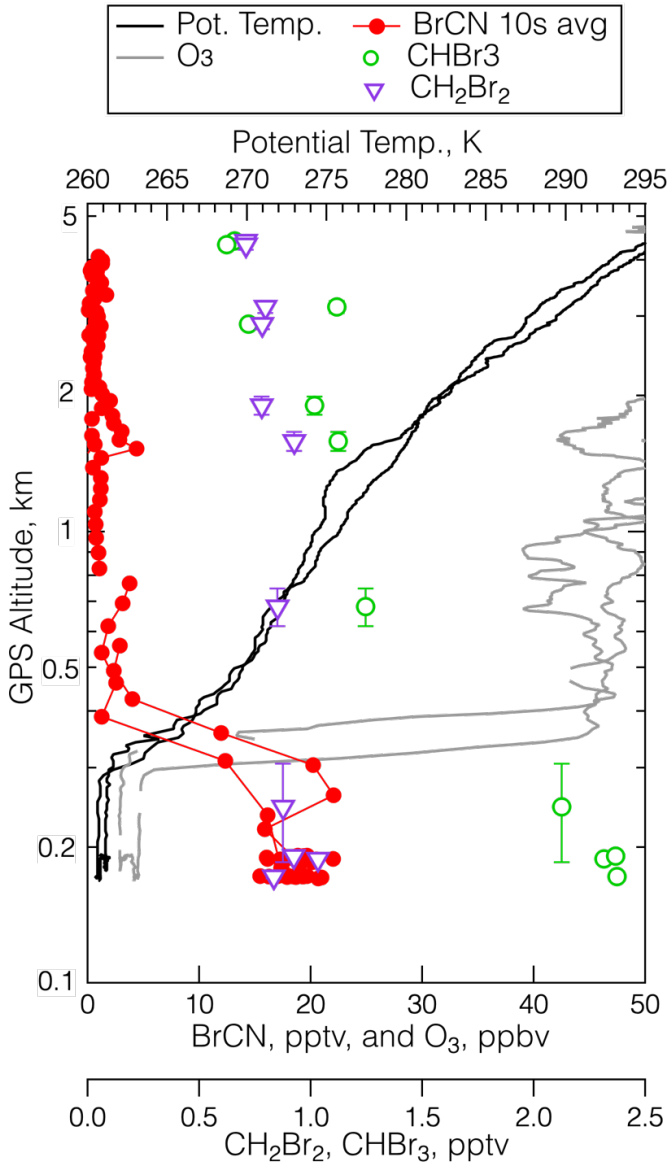

Figure 11. The vertical distribution of BrCN (red dots), O_3 (grey), $CHBr_3$ (blue open circles), CH_2Br_2 (purple triangles), and potential temperature (black) during the low-level leg at 22:30 UTC on May 19, 2018. The error bars are the standard deviation of the average altitude traversed during the WAS sampling time.